The Mount Pleasant Ore System: Result of A-type or Topaz-rhyolite Magmatism?

Andrew James Houston

November 25, 2019

GEOL 394

Advisors: Dr. Philip Piccoli, Austin Gion, Dr. Richard Ash

Abstract

Mount Pleasant is a magmatic-hydrothermal, tin-tungsten-molybdenum-indium ore system located in southern New Brunswick, Canada. Although the ore system has been well-described in past research and industry work, there are conflicting interpretations of the characterization of the host granite: is the Mount Pleasant system the result of A-type or topaz-rhyolite magmatism? To further investigate this geologic question, the minerology, major element, and trace element concentrations of trioctahedral micas in Mount Pleasant will be compared to the other trioctahedral micas in rocks from localities of a known origin. In this study, the types with a known origin will be A-type granites from Climax, CO, USA, and topaz-rhyolites from Thomas Range, Utah, and Pine Grove, Utah. The accessory phases in this study are trioctahedral micas (such as biotite or zinnwaldite) and these were chosen because they are common to the three systems of interest and their geochemical signatures can be used as petrogenic indicators of other ore systems. Thin sections from Mount Pleasant, Climax, Thomas Range, and Pine Grove were obtained and petrography was performed on the sections to identify the phases of interest. These phases were then analyzed by electron probe microanalysis and laser ablation inductively coupled plasma mass spectrometry to determine the major and trace element compositions of the phases. Mount Pleasant contained the trioctahedral mica zinnwaldite, and the trioctahedral mica biotite was identified in at least one thin section from Climax, Thomas Range, and Pine Grove. The Mount Pleasant zinnwaldites are enriched in Li, Rb, and F, and are very magnesium poor. The topaz-rhyolite biotite from Thomas Range and Pine Grove are both enriched in F and Ti but the two Thomas Range localities differ in Fe/Mg ratios and Mn content. All of the topaz-rhyolites are depleted in Li. The Climax biotite have weight percent levels of Ti, Mn, and F and some of the samples had low, but still significant levels of Li. The composition of Mount Pleasant trioctahedral micas differed from both the A-type and topaz-rhyolites, however, Mount Pleasant tended to be closer to Climax (A-type) than Thomas Range or Pine Grove (topaz-rhyolite). To statistically analyze the data and directly test the hypotheses, F and T tests were performed for criteria that distinguishes the different types of magmatism between the different trioctahedral micas. The criteria used were the Li, Rb, Zr, La, and Lu contents, as well as the ratio X_{Ann}^{Bt}.Other than Lu, which is statistically indistinguishable at the 0.05 level of significance between all the sites, only Climax showed additional similarities to Mount Pleasant. This includes the X_{Ann}^{Bt}, and while not actually statistically different, the La content was very close to being similar (at the 0.05 level it's different but it is statistically indistinguishable at the 0.047 level). Despite these similarities, other key variables such as Li, Rb, Zr are different between Mount Pleasant and Climax. As such, the type of magmatism that formed Mount Pleasant cannot be definitively constrained as A-type or topaz-rhyolite, though it may be more similar to Climax (A-type).

Introduction and Background

The Mount Pleasant ore system is located in southern New Brunswick, Canada (Figure 1). The system consists of two distinct deposits: the tungsten-molybdenum Fire Tower Zone and the indium-tin North Zone (Sinclair et al., 2006). Although there has been research conducted examining the geology of Mount Pleasant and its formation, there is a disparity in the interpretation of the type of magmatism that formed the deposits. Sinclair et al. (2006) suggest that Mount Pleasant has a topaz-rhyolite origin due to the presence of primary topaz and whole rock chemical data. Conversely, Inverno and Hutchinson (2006) suggest an A-type genesis due

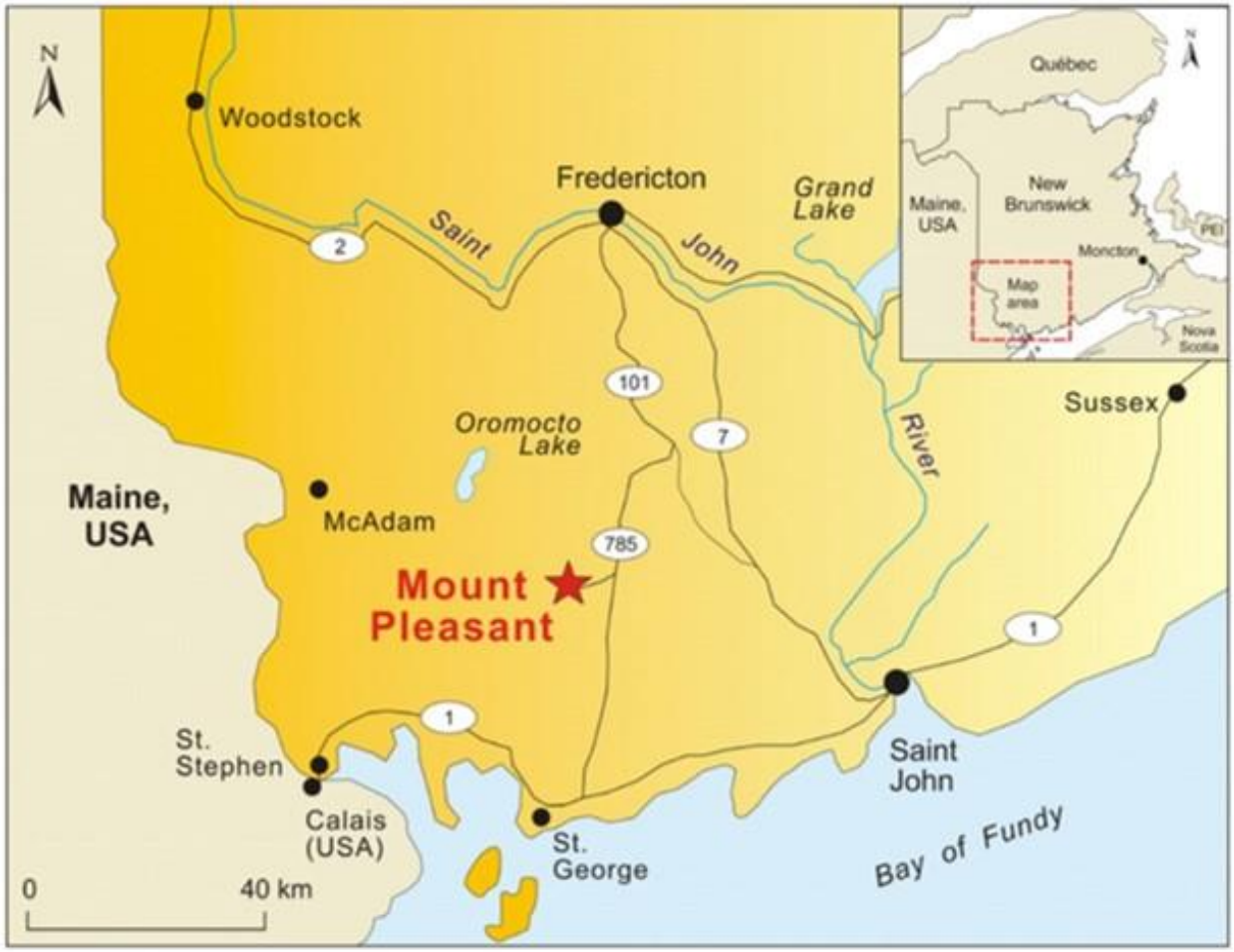

Figure 1. Location of Mount Pleasant. http://www.adexmining.com/aboutcompany.php

to petrographic, textural, and trace element characteristics that are indicative of A-type magmatism. To provide insights and possibly resolve this geologic question, characteristics of Mount Pleasant will be compared to two sites of a known magmatic type: A-type granites from Climax, CO, USA, and topaz-rhyolites from Utah, USA.

Mount Pleasant started as a joint venture between Billiton Exploration Canada Ltd. and Brunswick Tin Mines Ltd. and was initially mined for tungsten which began operation in 1983 (ADEX 2014). Production stopped after a drop in tungsten prices, and although it was evaluated for tin resources, tin mining was not economically feasible at the time. Mount Pleasant was sold to ADEX in 1995, which has been preparing for the past two decades to reopen the mine (ADEX 2014). The Mount Pleasant deposits are hosted within rocks of the Late Devonian Piskahegan Group, which includes layers of rhyolitic ash flow tuffs, sedimentary breccia, and a rhyodactic

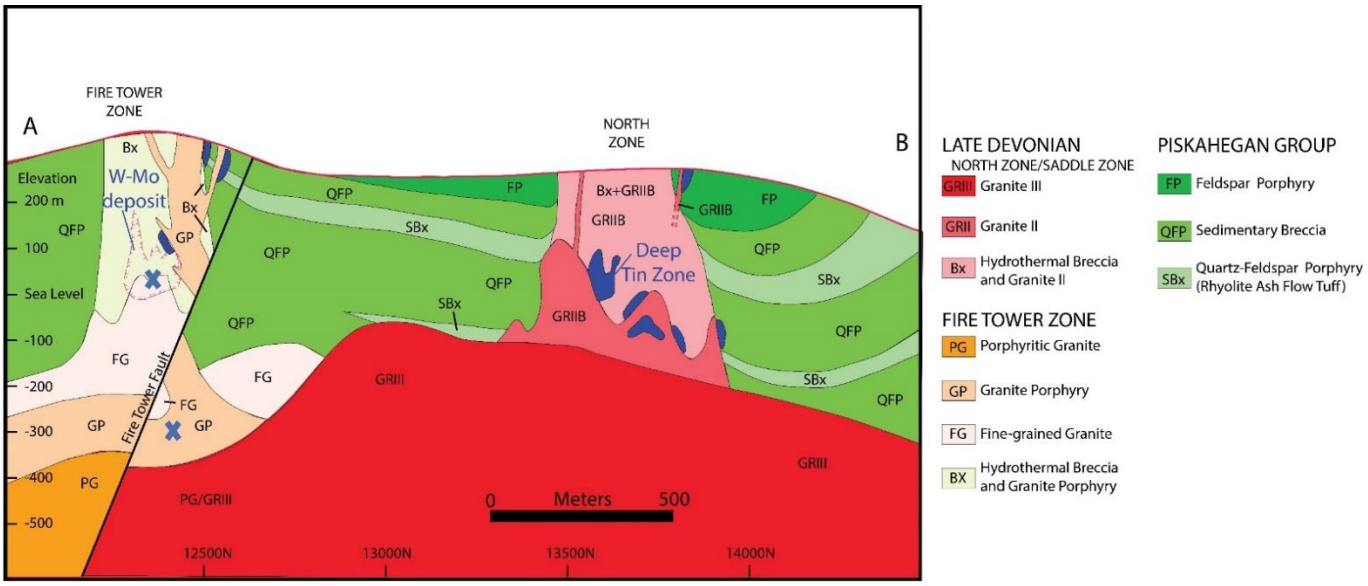

Figure 2. Geologic Cross Section of Mount Pleasant. Areas where samples were collected from are marked with an 'X'. Modified from Sinclair et al. (2006).

flow of feldspar porphyry (Sinclair et al., 2006). These rocks have been intruded several times by felsic magmas, which are now granites (Figure 2). There are three stages of granitic intrusions and two of them are associated with ore mineralization. There are two distinct ore zones at Mount Pleasant: the Fire Tower Zone and the North Zone. The Fire Tower Zone consists of porphyry tungsten-molybdenum deposits and the North Zone consists of indium-bearing tin deposits (Sinclair et al., 2006). This study is focused on Fire Tower Zone which comprises a hydrothermal breccia (Bx), fine-grained granite (FG), and granite porphyry (GP) units. The ore samples from Mount

Table 1. Mount Pleasant Samples

Sample no.	Rock type	Sample Site
MP-91-1.8	Stockwork Ore	collected from trench in stockworks
MP-91-1.16	Silicified Granite	
MP-91-1.18	Chloritized Granite	
MP-91-1.19	Sulfide Ore	
MP-91-1.20	Biotite Hornfels	collected from sedimentary breccia host rocks
MP-91-1.46	Sulfide Ore	
MP-91-1.48	Greisen/Stockwork Veins	
MP-91-1.21	Granite Porphyry	drill core from hole B-10 in Firetower Zone; collected at 11 foot depth from surface
MP-91-1.36	Barren Granite	drill core from hole B-156 in Firetower Zone; collected from a depth of 1538 feet from surface

Information regarding samples obtained from Mount Pleasant. The causative pluton sample utilized by this study is MP-91-1.36.

Pleasant utilized in this study were collected from the deposit, and the causative pluton samples were collected from the granite porphyry (Table 1). The modal mineralogy of granite porphyry is 68.28% K-feldspar and 26. 15% quartz for the major phases, and for the accessory phases of interest, 4.14% biotite and 0.24% fluorite (Inverno and Hutchinson 2006). Although primary topaz was identified at Mount Pleasant by Sinclair et al. (2006), Inverno and Hutchinson (2006) failed to find any in the thin sections they obtained, likely due to their limited sampling area (Sinclair et al., 2007). Mount Pleasant, although historically mined for tungsten, has appreciable, and potentially economic, deposits of molybdenum. In Figure 3, molybdenum deposits are

Figure 3. Map of molybdenum deposits across the United States. Modified from Wallace (1985).

mapped across the continental United States and a part of New Brunswick, Canada. The sites

plotted on the map are the sample sites being utilized by this study; it is a subset of the sites that were originally included. Wallace (1985) grouped the deposits into two categories: Climax-type and sub-Climax-types. This classification is based on the ore grade. Climax-types contain an average of 0.35 to 0.45 percent MoS_2 and do not go below 0.20 percent (Wallace 1985). Sub-Climax types contain a lower percentage of MoS_2, commonly one-half to one-quarter of Climax-types, but still have characteristics of Climax-types such as anomalous fluorine (Wallace 1985). Of the sites in Figure 3 all except Climax are sub-Climax-type, while Climax is Climax-type. The vast majority of the deposits are located in the western United States, with the exception of Mount Pleasant. It is worth noting that Mount Pleasant is in a completely different location and therefore also has a very different geologic history compared to those in the western United States. That being said, this map connects Mt. Pleasant to these other deposits due to similarities in deposit type and grade making them good comparison sites between Mt. Pleasant and other sites that are representative of A-type and topaz-rhyolites. Climax, CO, USA, is well known to be an A-type granite and is the type-locality for the other climax deposits around it (Audétat and Li 2017). The topaz-rhyolites of Utah, which for the purposes of this research are composed of the rhyolites from Thomas Range and Pine Grove, are the result of topaz-rhyolite magmatism.

Climax is an open-pit mine approximately 13 miles from Leadville, CO, and consists of a porphyry molybdenum deposit with molybdenite as the primary ore mineral (Climax Molybdenum Company, 2013). The mine is one of two molybdenum mines in Colorado owned

Table 2. Climax Samples

Catalog Number	Type	Number	Notes
EGR.719R	Porphyry	T-2	The first pulse of the Climax stock was the intrusion of the Southwest Mass. The hydorthermal event that followed gave rise to the Ceresco Ore Body. This ore formed 700 feet to 2,000 feet above and peripheral to the parent Southwest Mass. Sample T-2 was collected along the south boundary of the Southwest Mass approzimately 300 feet below Ceresco ore, and outside the Upper and Lower Ore Bodies. As a result, the rock is relatively fresh and contains only 0,06 percent molybdenite.
EGR.720R	Porphyry	T-3	The Central Mass of the Climax Porphyry was forcefully intruded as the second igneous pulse and was followed by a hydrothermal event which gave rise to the Upper Ore Body. The rock is predominately rhyolite porphyry, but varies considerably in texture from rhylotie to porphyritic granite. The elongated quartz eyes provide evidence of forceful intrusion. Sample T-3 was collected 260 feet below the Phillipson Level in an area where the Upper and Lower Ore Bodies are superimposed. As a result, the sample exhibits well-developed stockwork veining typical of Climax ore. Sample T-3 contains more than 0.5 percent molybdenite.
EGR.721R	Porphyry	T-4	Rock sample T-4 is termed "Salt and Pepper" rock because of the disseminated biotite. The rock represnts what is believed to be the major rock type of the Aplite Porphyry plug, if indeed there is a plug. The origin and exact location of the Aplite Porphyry plug can only be assumed because of the lack of information from the deeper mine levels. There is a possibility that the "Salt and Peppper" rock represents dikes radiating out from a plug unexposed at depth. "Salt and Pepper" rock is cut by Lower Ore Body molybdenite and Lower Ore Body High Silica Rock. Sample T-4 is cut by barren quartz veins along which bleaching has occurred; it contains about 0.4 percent molybdenite.
EGR.722R	Porphyry	T-5	Sample T-5 was taken from an Intra-Mineral Dike. The Intra-Mineral Dikes cut Upper Ore Body molybdenite and Upper Ore Body High Silica Rock, and are cut by Lower Ore Body molybdenite and High Silica Rock. These dikes radiate out from a center on the Phillipson and White Levels. Below the Phillipson Level the dikes thin out and cannot be traced to a definte source rock. THe Aplite Porphyry plug is probably the source rock. Sample T-5 is stongly silicified, probably by Lower Ore Body quartz-topaz mineralizaion peripheral to the Lower Ore Body molybdenite.
EGR.723R	Granite	T-6	Sample T-6 was collected from the Late Core or Porphyritic Granite phase of the Climax stock. This intrusive event was the fourth and last major igneous pulse recognized in the mine. Although the Late Core rock is referred to as Porphyritic Granite phase of the Climax stock. This intrusive event was the fourth and last major igneous pulse recognized in the mine. Although the Late Core rock is referred to as a Porphyritic Granite, sample T-6 is a rhyolite porphyry with a very fine-grained groundmass.Except for minor disseminated molybdenite seen in some samples, the Late Core rock is characteristically barrenn of mineraliztions.
EGR.725R	Granite	T-7	The late core pegmatitie clearly cuts the Porphyritic Granite Phase. The pegmatite is probably related to a hydrothermal pulse which is related to the barren Core Phase. Minor disseminated sphalerite, chalcopyrite, rhodochrosite, fluorite, huebnerite, and molybdenite found in the pegmatite indicate that ore minerals were present during the last igneous event.

Descriptions of Samples from Climax, CO. Modified from Wallace et al., 1968, and information provided by the Denver Museum of Nature and Science.

by the Climax Molybdenum Company, the other being the Henderson underground mine. Both of these produce molybdenum concentrates: higher purity from Henderson and lower purity from Climax. From the mines, the molybdenum is either sold as-is or further processed off-site (Climax Molybdenum Company, 2013). The granites at Climax that are thought to be the

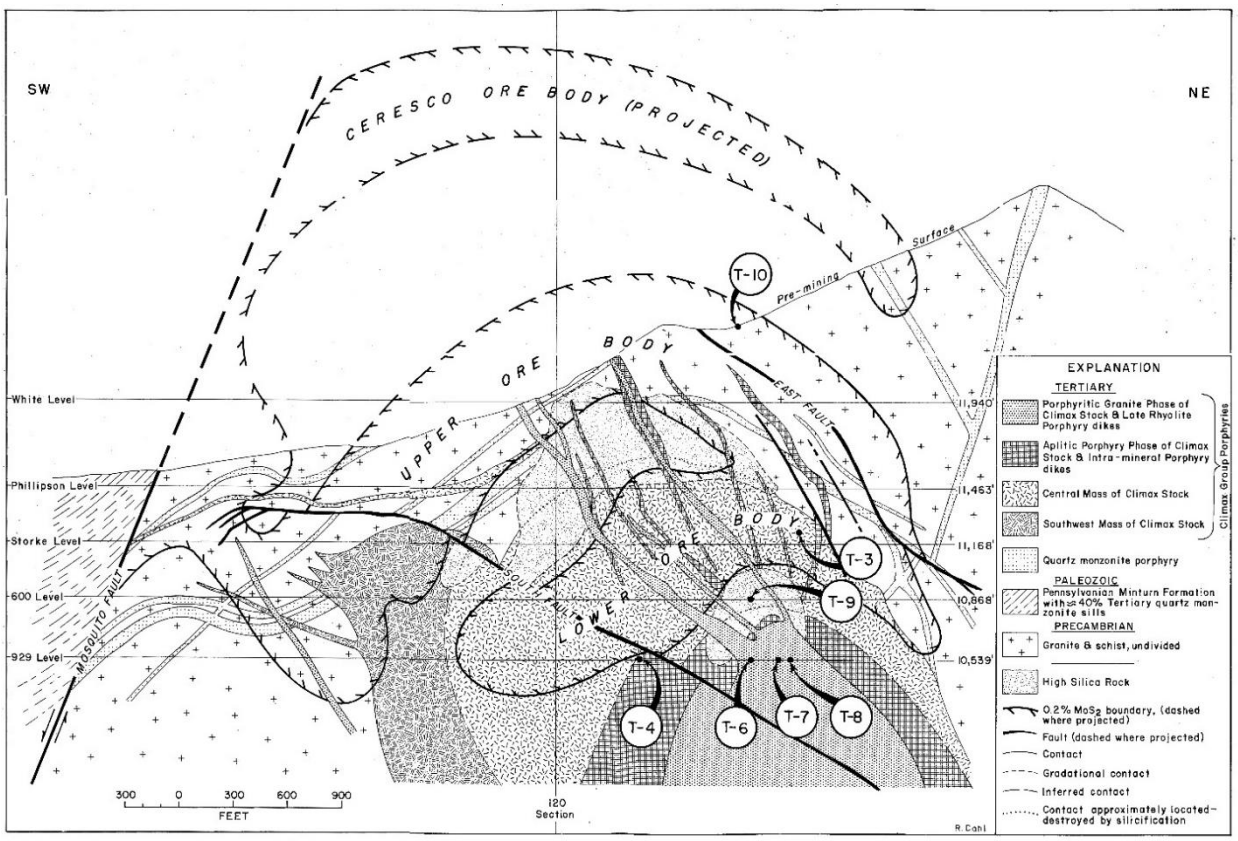

Figure 4. Locations of sample retrieval sites within the Climax ore system. Table 2 contains descriptions of several of these samples. Modified from Wallace et al., 1968.

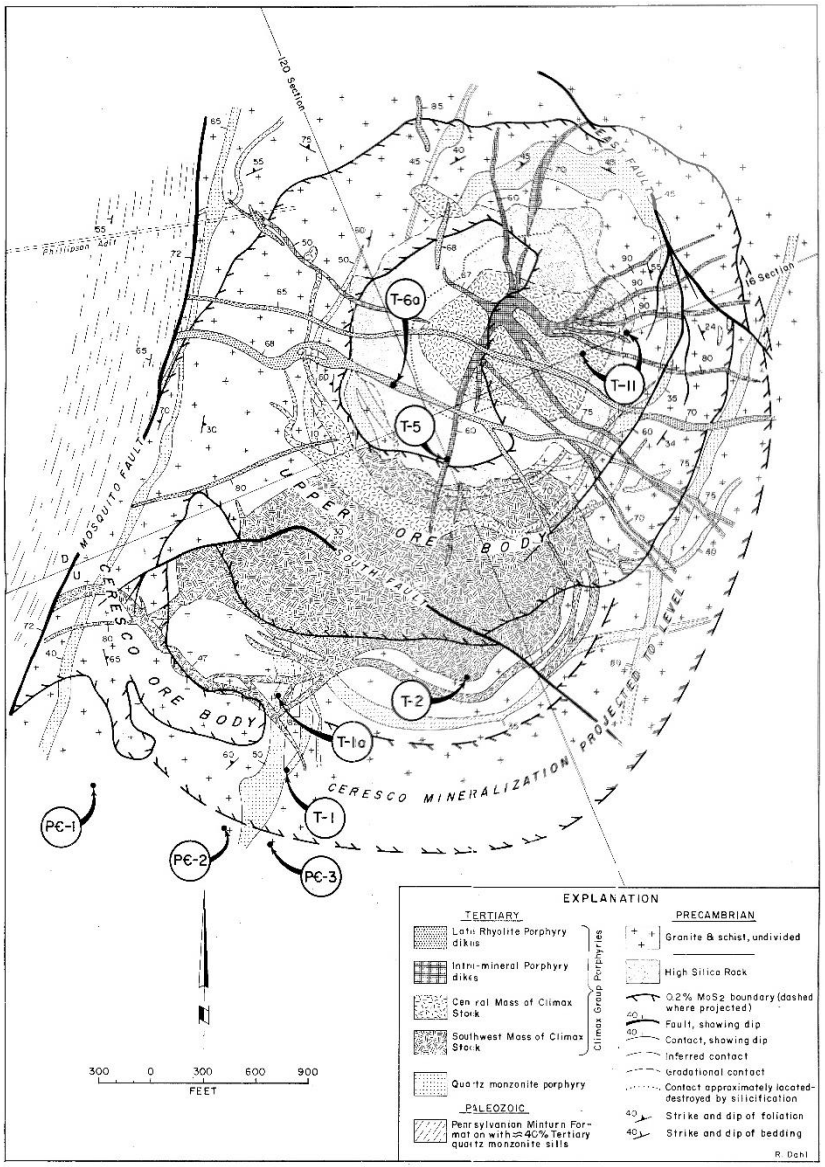

Figure 5. Locations of additional sample retrieval sites within the Climax ore system. Table 2 contains descriptions of several of these samples. Modified from Wallace et al., 1968.

magmatic origin of the ore deposit are A-type granites with high concentrations of fluorine and water (Audétat and Li 2017). The Denver Museum of Nature and Science provided rock samples from Climax from which thin sections were cut (Table 2). Figures 4 and 5 illustrate where the samples in table 2 were collected from within the ore system.

The topaz-rhyolites of Utah that are being examined in this study are the ones found in the Thomas Range and at Pine Grove. Although volcanic in origin, these rocks are analogous to topaz-granites compositionally and can be treated as such (Clemens et al., 1986). Both localities are part of a larger group of Cenozoic topaz-bearing, high silica rhyolites distributed across the western United States. Common characteristics of these topaz-rhyolites are that they are enriched in fluorine, contain post-magmatic vapor-phase topaz, and almost always occur as small lava domes with or without flows (Christiansen et al.,1986).

Table 3. Topaz-rhyolite Samples

Sample	Unit Type	Unit Description	Coordinates
109593-10	Primary rhyolite from Juab County	Rhyolite from near top of 5th major subgroup of the younger volcanic group. Collected on falt upper surface about 2000ft east of peak 7046 on Topaz Mountain	NW SW sec. 9, T. 13 S., R.11 W.
109593-13	Primary porphertic rhyolite from Juab County	Porphyritic rhyolite from hill 5467 at south end of Thomas Range in the NE corner of sec. 21, T. 13 S., R.11 W. This hill is a volcanic neck.	NE sec. 21, T. 13 S., R.11 W.
Pine 2 Tpg	Pine Grove porphery	Strongly Weathered Pine Grove porphery , taken close to road	38 20.20'N 113 36.58'W
Pine 7 Tbpa	Air fall unit	N/A	38 21.90'N 113 29.99'W

Information regarding the samples obtained from topaz-rhyolite localities used in this study. Samples acquired from Leslie Hale and Dr. Andreas Audétat. Modified from Staatz and Carr (1964).

The Thomas Range, located in west-central Utah, is host to well-known topaz-rhyolite flows and is associated with nearby U, Be, and F deposits. The flows are of varying ages and the samples used in this study range from 6 m.y.-38 m.y. Pine Grove, and its associated porphyry molybdenum deposit, is located in the Wah Wah mountains, and is approximately 24 m.y. (Christiansen et al.,1986). Table 3 contains all the topaz-rhyolite samples utilized in this research and details about each one.

All the localities included in this study are thought to be related to magmatic-hydrothermal ore systems, and as such have similar methods of formation. The residing theory for their formation is laid down in the magmatic-hydrothermal theory for the formation of porphyry ore deposits (Hedenquist and Lowenstern 1994). This theory can be summarized as follows (Figure 6). A felsic intrusion is emplaced at shallow levels in the crust, commonly no deeper than 6 km. The magma starts to cool, and crystallization of phases such as quartz and feldspar begins to occur on the outer rims of the emplaced magma. These phases, especially quartz, do not have significant, if any, amount of ore metals (such as Mo, W, In, or Sn) as it is difficult to have those elements to substitute into their crystal structure. This, and the fact that the minerals crystalizing are anhydrous, causes the concentration of the ore metals and water (H_2O trapped in the structure of the melt) to increase. At a certain point, which depends on the temperature and pressure of the system, a volatile phase, consisting of mostly water plus some ore metals and other elements (Na, K, Ca, Fe), will exsolve. The changing temperature conditions causes these phases to no longer be stable. This new volatile phase rises through the crust due to its lower density, often by following faults or cracks in the subsurface geology. It can rise all the way to the surface or, more commonly, get in trapped in cupolas: dome-like structures above igneous intrusive bodies. Regardless of which path it takes, the volatile phase cools, and the ore-bearing minerals will precipitate. The alphabet classification of granites was proposed by Chappell and White (1974) who divided granites into two types: I-type and S-type. Chappell and White derived their classification method by examining granites of major batholiths in the Tasman Orogenic Zone of eastern Australia. Loiselle and Wones (1979) categorized another distinct group of granites, the A-types.

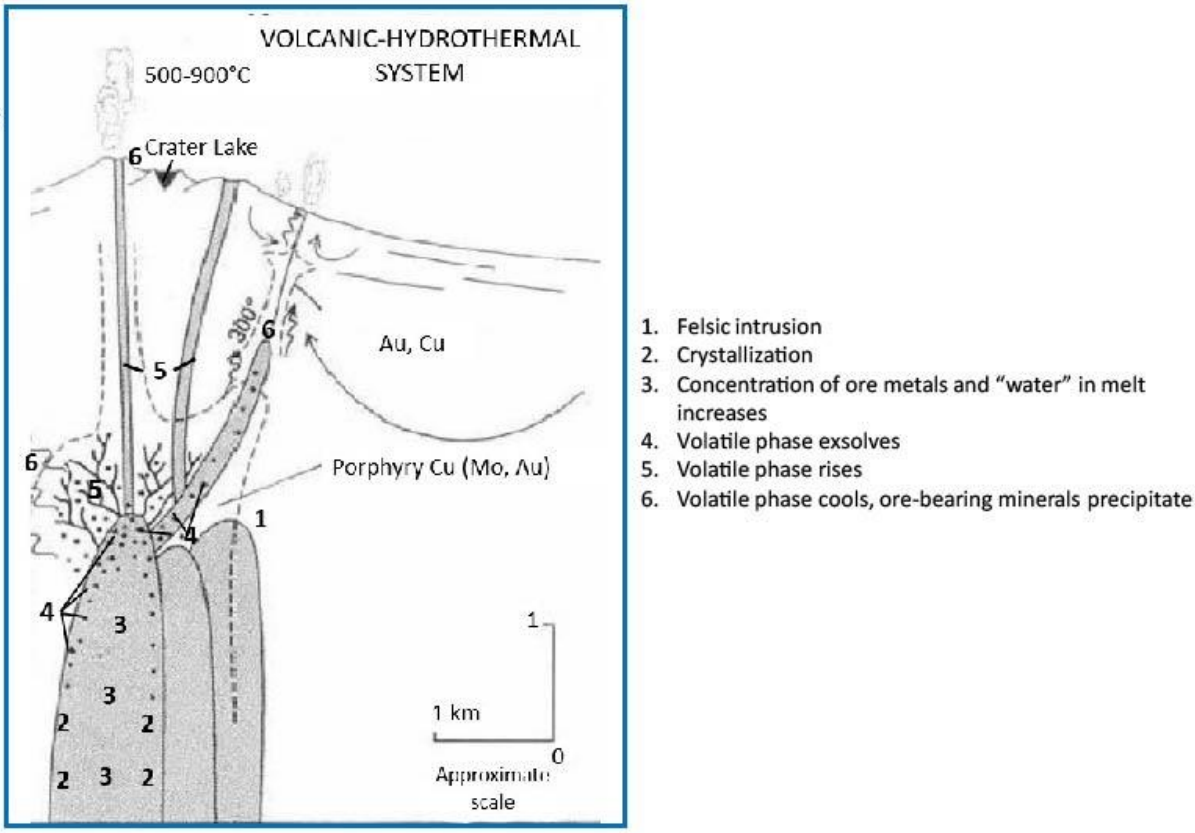

Figure 6. Diagram Depicting the hydrothermal-magmatic theory for the formation of porphyry ore deposits. Modified from Hedenquist and Lowenstern (1994).

Table 4 compares the chemical and mineralogical characteristics of these three types. I-type and S-type, are classified based on their source: I standing for preexisting igneous source and S standing for preexisting sedimentary source. One common deposit associated with I-types are porphyry copper deposits, and one common to S-types are porphyry tin deposits. A-types, which can stand for anorogenic, alkaline and/or anhydrous depending on the paper and author, are not classified based on source (Clemens et al. 1986). Topaz-rhyolites are associated with A-type magmatism; however, they are different and are sometimes considered a subclass of A-types (Clemens et al. 1986). Differences include temperature of formation, mineralogy, and trace element chemistry (Table 5).

Table 5. A-type vs topaz-rhyolites

Feature	A-type	Topaz-rhyolite
T	High	Low to Moderate (600-800°C)
REEs	High	Moderate LREE, high HREE
Enriched	Zr	Li, U, Th, Rb
Depleted	Ni	Zr
Mineralogy	Sodic-amphiboles, olivine	

Distinguishing characteristics of A-types and topaz-rhyolites. Modified from Christiansen et al. (1983)

	Type	SiO_2	K_2O/Na_2O	$A/(C+N+K)^*$	Fe^{3+}/Fe^{2+}	Mineralogy	Trace Element Chemistry	Petrogenesis
Source-based classification	**I**	53-76%	Low	Low: metaluminous to peraluminous	Moderate	Hornblende magnetite	High LIL, high HFS medium Rb, Th, U	Subduction zone, infracrustal, Mafic to intermediate. Igneous source
	S	65-74%	High	High: peraluminous	Low	Muscovite, cordierite, alumino-silicates, garnet, ilmenite	Variable LIL/HFS high Rb, Th, U	Subduction zone, supracrustal sedimentary source
Other classification	**A + Topaz-rhyolites**	High >77%	Na_2O high (K_2O+Na_2O)	Variable: peralkaline	Variable	Topaz, fluorite, sodic-amphiboles, olivine	Low LIL/HFS, high Fe/Mg, high Ga/Al, high REE, Zr, high F, Cl	Anorogenic, stable craton, rift zone

Table 4. Subset of the Alphabet classification of granites. Modified from Chappell and White (1974), Loiselle and Wones (1979), and Clemens et al. (1987)`

The main objective of this research is to determine whether Mount Pleasant is more similar to the topaz-rhyolites of central Utah or the Climax A-type granites and to characterize the major and trace elements in trioctahedral micas in the Mount Pleasant system. Trioctahedral micas were chosen as the phases of interest since they are common to all the sample sites and that they can be used as provenance indicators. A trioctahedral mica is a phyllosilicate where each O or OH (or common substitutions such as F or Cl) ion is surrounded by 3 divalent cations. These include the annite-phlogopite (biotite) solid solution $KFe_3AlSi_3O_{10}(F,OH,Cl)_2$ - $KMg_3AlSi_3O_{10}(F,OH)_2$ and the siderophyllite-polylithionite solid solution $KFe_2AlAl_2Si_2O_{10}(F,OH)_2$ - $KLi_2AlSi_4O_{10}(F,OH)_2$. Abdel-Rahman concluded that biotite compositions largely depend on characteristics of the source magma and can be used as a proxy for the magmatic origin. Abdel-Rahman created an FeO-MgO-Al_2O_3 biotite discriminant diagram that can be used to display compositions of biotite and those compositions are indicative of the composition of magma (Figure 7). This research was later built upon and expanded this concept to include that other trioctahedral micas, not just biotite, can be used as indicators of provenance (Shabani et al. 2003).

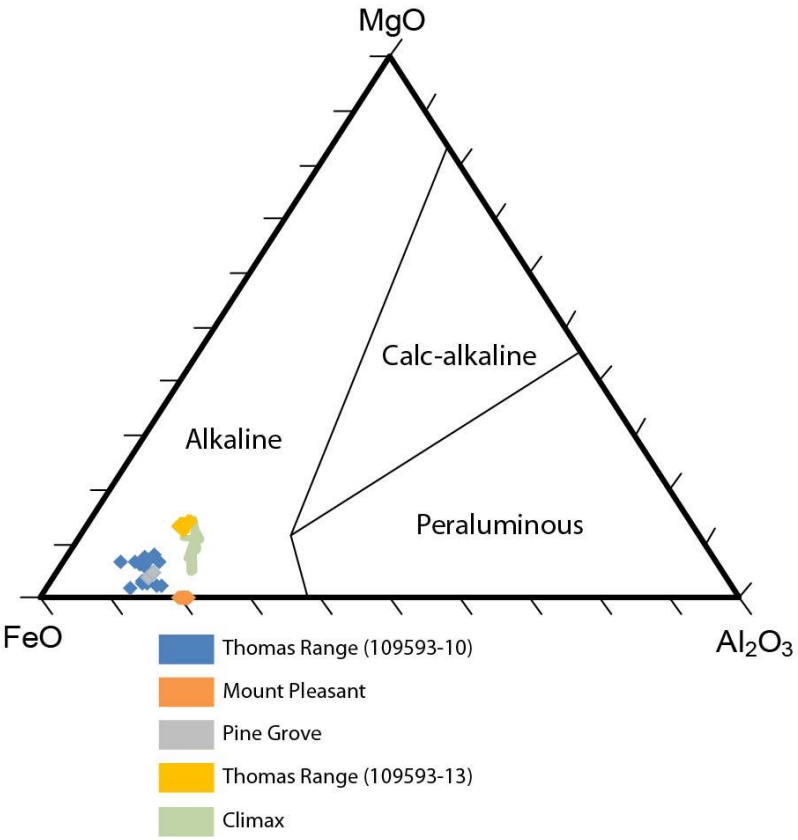

Figure 7. Biotite discriminant diagram. Axes in weight % oxide. Alkaline, calc-alkaline, and peraluminous are analogous to A, I, and S-type, respectively. Note that all samples used in this study plot in the alkaline, or A-type, field. Modified from Abdel-Rahman (1994).

The null hypothesis is there is no difference in the major and trace element signatures in the trioctahedral micas in the rocks from Mt. Pleasant, Climax, and the topaz-rhyolites of Utah.

Alternatively, the hypothesis is there is a difference in the major and trace element signatures in the trioctahedral micas in the rocks from Mt. Pleasant, Climax, and the topaz-rhyolites of Utah.

Methods

In order to test the hypotheses, the mineralogy of the granites and the chemistry of the trioctahedral micas will be compared between samples from Mount Pleasant to samples from the Climax A-types and the topaz-rhyolites of central Utah.

To determine the minerology and identify the trioctahedral micas and other phases of interest for later quantitative analysis, optical microscopy was performed on two thin sections from Mount Pleasant, six from Climax and four from the topaz-rhyolites of Utah. Trioctahedral micas were located in at least one thin section from each of the sample sites (Figure 8).

To examine the major element chemistry of the accessory phases in the samples, analyses were completed using an Electron Probe Microanalyzer (EPMA). The EPMA works by bombarding the surface of a sample (commonly a polished a thin section) with an electron beam. The electrons in the beam collide with those in the atoms of inner shells of elements in the sample, leaving vacancy for an electron in an outer shell to fill. This releases energy in the form of x-rays, which are characteristic of the element that released it. There are several detectors in the EPMA which can collect either x-rays or electrons. The electrons are collected for back-scatter

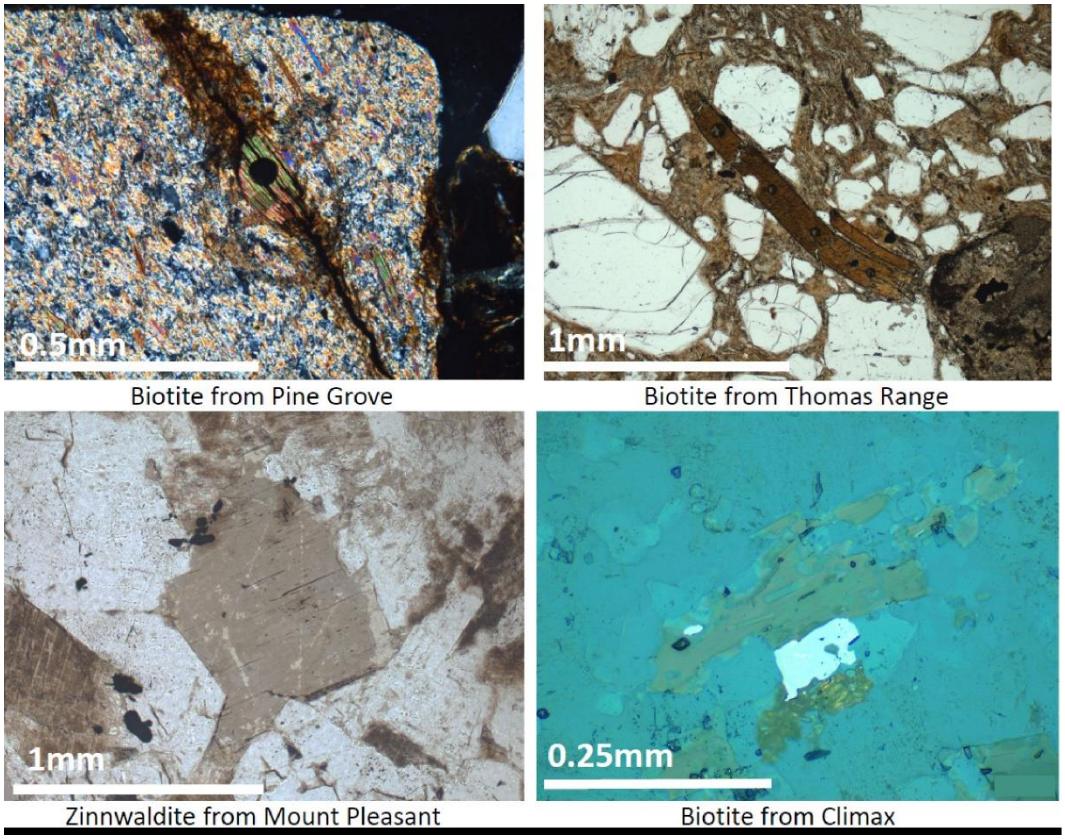

Figure 8. Photomicrographs of trioctahedral micas. Pine Grove biotite from sample Pine 7 Tbpa, Thomas Range biotite from sample NMNH-109593-13, Mount Pleasant zinnwaldite from sample, MP-91-1.36 and Climax biotite from sample 721r.

electron (BSE) imaging, wherein the higher the mean atomic number of the phase, the brighter

Table 6. EPMA Standards

				Count Times (sec)		
	Element	X-ray Line	Analytical Crystal	Peak	Background	Biotite Standards
1	Si	Kα	TAP	15	5	Kakanui Hornblende
2	Ti	Kα	PET	20	5	Kakanui Hornblende
3	Al	Kα	TAP	10	5	Kakanui Hornblende
4	Fe	Kα	LiF	30	5	Kakanui Hornblende
5	Mn	Kα	LiF	20	5	Rhodonite
6	Mg	Kα	TAP	20	5	Kakanui Hornblende
7	Ca	Kα	PET	20	5	Kakanui Hornblende
8	Na	Kα	TAP	20	5	Kakanui Hornblende
9	K	Kα	PET	20	5	Microcline
10	Rb	Lα	TAP	30	5	SPI-Pollucite
11	F	Kα	TAP	60	10	Topaz
12	Cl	Kα	PET	40	10	Scapolite

Electron Probe Microanalyzer standards. All analyses performed with an accelerating voltage of 15 kV, a cup current of 10 nA, and a beam diameter of 10 microns.

that phase looks. BSE imaging is used to locate minerals of interest. There are two main types of analysis that are performed using the EPMA, energy dispersive spectrometry (EDS) and wavelength dispersive spectrometry (WDS). EDS is a qualitative analysis where the characteristic x-rays are absorbed by a Si (Li) detector that measures the energy of the x-ray. These data are collected and plotted on graph of x-ray counts vs energy (keV). EDS is a first-order analysis that identifies the major elements and the approximate relative proportions of the elements in a phase being analyzed. It is commonly used to clarify what the phase is before moving on to a more quantitative analysis. WDS also utilizes the x-rays released by the interaction of the electron beam and the surface of a sample. Analytical crystals with specific lattice spacings are used so that when the incoming x-rays are diffracted, the position of each x-ray is known, and can be counted by a detector. Where to place the detectors is determined using Bragg's law [$n\lambda = 2d\sin\Theta$] with n being the order of reflection, λ the wavelength of incident x-rays, d the spacing between lattice planes, and Θ being the incident angle. All atoms of a given element have different spacings of orbitals, so each element produces x-rays at certain wavelengths based on the energy of the x-ray. The crystals have a fixed d-spacing and change location to satisfy Bragg's law when analyzing different elements.

To examine the trace element chemistry of the accessory phases in the samples, analyses have been completed utilizing a Laser Ablation Inductively Coupled Plasma Mass Spectrometer (LA-ICP-MS). This instrument works by first ablating the surface of a section with a focused laser beam. This removes a portion of the phase being targeted, which is subsequently entrained in a helium gas and carried to the mass spectrometer. This collection of helium and particles are then combined with argon gas and ionized by an argon plasma. An electromagnet controls an electrical and magnetic field that reflects ions of a specific atomic mass and then charged plates pull the ions to the detectors. To switch between measuring different isotopes, the current to the electromagnet is changed. The isotopes being analyzed in this study are ^{6}Li, ^{7}Li, ^{9}Be, ^{27}Al, ^{29}Si, ^{43}Ca, ^{45}Sc, ^{53}Cr, ^{67}Zn, ^{69}Ga, ^{85}Rb, ^{88}Sr, ^{89}Y, ^{90}Zr, ^{93}Nb, ^{97}Mo, ^{111}Cd, ^{115}In, ^{118}Sn, ^{133}Cs, ^{139}La, ^{140}Ce, ^{141}Pr, ^{146}Nd, ^{147}Sm, ^{151}Eu, ^{155}Gd, ^{157}Gd ,^{159}Tb, ^{163}Dy, ^{165}Ho, ^{166}Er, ^{169}Tm, ^{172}Yb, ^{175}Lu, ^{178}Hf, ^{181}Ta, ^{183}W, ^{232}Th, and ^{238}U. The standards used, which are analyzed before and after each

block of analyses, are NIST610 and BHVO2G. Each of the thin sections analyzed on the EPMA with the exception of Climax samples 719r, 720r, and 725r were analyzed on the LA-ICP-MS and as many of the same grains were analyzed as possible. The raw data from the LA-ICP-MS analyses were reduced using the LAMTRACE data reduction software (Jackson 2008).

To statistically analyze the data and directly test the hypotheses, F-tests and t-tests were performed for criteria including, but not limited to, several of the distinguishing characteristics of A-types and topaz-rhyolites from table 5. The procedure for this consisted of using an F test to determine whether the variances of two different groups were similar or different for a given variable, and then using the corresponding test to determine whether the two groups were statistically undistinguishable or not.

Uncertainties were calculated in the same manner for EPMA and LA-ICP-MS. Uncertainty on a single analysis is due to counting statistics. Means were taken for each phase of each of sample and the standard deviation of the mean ($\sigma_m = (\sqrt{\sum(x - \overline{x})^2/(N-1)}\ /\ \sqrt{N})$ was calculated for each of those phases. These standard deviations of the means were then plotted as error bars on the means. If the biotite from the same sample were analyzed again, the mean and standard deviation of the mean represent a prediction where the data from the next analysis would be.

Data

WDS analyses were successfully completed for phases of interest in thin sections from Mount Pleasant, the topaz-rhyolites from Thomas Range and Pine Grove, and Climax. Mineral formulas for micas were calculated on the basis of 11 oxygens and based on the method described in Nesse 2016.

Trioctahedral micas were analyzed for major element data in Mount Pleasant sample MP-91-1.36 (Table 7). The calculated mineral formulas are zinnwaldite, a Li-bearing trioctahedral mica of the formula $KLiFeAlAlSi_3O_{10}(F,OH)_2$. These zinnwaldite are also very magnesium-poor and enriched in rubidium and fluorine. Grains of topaz and fluorite were also analyzed but as neither of the phases appear in any other samples these analyses were not used in this study and are in appendix Tables A.2 and A.3 for completion sake. Trioctahedral micas were analyzed for major element data in Thomas Range samples NMNH 109593-10 and NMNH 109593-13 and Pine Grove sample Pine 7 Tbpa (Table 8). Pine Grove sample Pine 2 Tpg was also analyzed but only muscovite (a dioctahedral mica) was present and these analyses are reported in appendix Table A.4. All the trioctahedral micas in the topaz-rhyolites were calculated to be biotite, which has the basic formula K(Mg, Fe)3AlSi3O10(OH,F)2. NMNH 109593-10 has a high Fe/Mg ratio, weight percent levels of manganese and titanium, and enriched in fluorine. NMNH 109593-13 is also enriched in fluorine and has weight percent levels of titanium but has little manganese and has lower Fe/Mg ratio. Pine 7 Tbpa has anomalous high levels of silicon and aluminum for a biotite. All the micas from the topaz-rhyolites are depleted in lithium.

Table 7. Mount Pleasant Major Element Trioctahedral Mica Analyses

Mount Pleasant					
	1(N=5)	**2(N=5)**	**3(N=5)**	**4(N=5)**	**5(N=6)**
SiO_2	42.2(0.2)	40.3(0.7)	41.5(0.2)	41.5(0.3)	41.2(0.6)
Al_2O_3	20.6(0.1)	20.7(0.2)	20.6(0.2)	20.7(0.2)	20.3(0.2)
TiO_2	0.4(0.1)	0.16(0.05)	0.5(0.07)	0.3(0.08)	0.2(0.03)
FeO	16.1(0.3)	14.6(0.2)	15.8(0.3)	15.6(0.3)	15.3(0.2)
MnO	1.4(0.06)	1.4(0.01)	1.5(0.1)	1.5(0.06)	1.5(0.06)
MgO	0.03(0.008)	0.05(0.01)	0.04(0.01)	0.03(0.006)	0.03(0.006)
Li_2O	2.5(0.07)	3.0(0.10)	2.84(0.09)	3.1(0.07)	3.2(0.10)
Rb_2O	1.9(0.09)	1.97(0.04)	1.8(0.07)	1.9(0.09)	2.0(.01)
CaO	BD	BD	0.01(0.009)	BD	BD
Na_2O	0.22(0.02)	0.25(0.04)	0.18(0.03)	0.3(0.03)	0.3(0.02)
K_2O	10.2(0.07)	9.7(0.1)	10.1(0.04)	9.6(0.08)	9.9(0.05)
Cl	0.01(0.003)	0.007(0.003)	0.01(0.002)	0.03(0.01)	.01(0.003)
F	5.3(0.2)	5.8(0.2)	4.9(0.2)	5.2(0.2)	5.7(0.08)
Total	*96(1)*	*92(1.7)*	*95(1)*	*94(1.1)*	*93(1.6)*
Mineral Formuals Calculated on the Basis of 11 Oxygens					
Si	3.055	3.011	3.049	3.050	3.042
Al	0.945	0.989	0.951	0.950	0.958
Al	0.816	0.837	0.833	0.841	0.809
Ti	0.022	0.009	0.026	0.019	0.012
Fe	0.977	0.915	0.972	0.956	0.946
Mn	0.084	0.088	0.091	0.092	0.093
Mg	0.003	0.006	0.004	0.004	0.004
Li	0.752	0.798	0.783	0.648	0.720
Rb	0.090	0.095	0.087	0.091	0.095
Ca	0.000	0.000	0.001	0.000	0.000
Na	0.032	0.036	0.026	0.039	0.040
K	0.940	0.930	0.947	0.904	0.934
Cl	0.001	0.001	0.001	0.004	0.001
F	0.607	0.681	0.575	0.603	0.663

Average major element analyses of Mount Pleasant and Thomas Range trioctahedral micas. Numbers across the top represent grain numbers. N represents the number of analyses. Top values in wt% oxides, bottom are mineral formulas in apfu. The numbers in parentheses represent the standard deviation of the mean (1σ). Li calculated using data from LA-ICP-MS analyses of the same grains. BD stands for below detection.

Table 8. Topaz-rhyolite Major Element Trioctahedral Mica Analyses

		Thomas Range (NMNH 109593-10)				Thomas Range (NMNH 109593-13)				Pine 7 Tbpa
	1(N=5)	2(N=1)	3(N=4)	4(N=2)	5(N=4)	1(N=2)	2(N=4)	3(N=3)	4(N=3)	1(N=2)
SiO_2	33.1(0.9)	35.64	33.2(1.3)	33(0.6)	32.5(0.07)	36.9(0.11)	36.1(0.32)	35.7(0.23)	36.0(0.77)	51.4(0.84)
Al_2O_3	12(0.5)	15.39	13(1.3)	13.5(0.4)	11.5(0.3)	13.7(0.32)	14.0(0.10)	14.0(0.10)	13.6(0.36)	25.9(0.44)
TiO_2	3.3(0.6)	2.34	2.8(0.4)	3.2(0.03)	3.1(0.03)	3.6(0.06)	3.5(0.05)	3.9(0.04)	3.5(0.04)	0.73(0.38)
FeO	30(1.6)	26.18	29(1.7)	31(1.3)	31(0.6)	16.4(0.36)	17.5(0.21)	17.9(0.24)	17.4(0.07)	4.4(0.09)
MnO	2.2(0.09)	3.14	2.5(0.3)	2.8(0.03)	2(0.1)	0.61(0.03)	0.60(0.03)	0.56(0.02)	0.62(0.05)	0.73(0.04)
MgO	7.1(0.2)	2.13	4.6(1.3)	2.9(0.1)	6.4(0.3)	13.4(0.46)	12.9(0.13)	12.8(0.34)	13.6(0.12)	1.5(0.05)
Li_2O										
Rb_2O	0.13(0.03)	0.16	0.3(0.1)	0.009(0.005)	0.09(0.02)	0.10(0.03)	0.07(0.02)	0.06(0.03)	0.1(0.002)	0.19(0.03)
CaO	0.08(0.01)	0.05	0.03(0.02)	0.1(0.01)	0.09(0.08)	0.09(0.07)	0.01(0.002)	BD	0.02(0.01)	0.14(0.01)
Na_2O	0.57(0.02)	0.69	0.54(0.05)	0.45(0.009)	0.44(0.02)	0.41(0.01)	0.40(0.02)	0.41(0.01)	0.40(0.004)	0.09(0.02)
K_2O	8.3(0.3)	8.99	8.3(0.2)	8.4(0.2)	8.4(0.06)	9.1(0.22)	9.1(0.10)	8.9(0.11)	9.4(0.04)	9.1(0.25)
Cl	0.22(0.02)	0.58	0.3(0.09)	0.2(0.01)	0.2(0.006)	0.08(0.002)	0.07(0.003)	0.07(0.003)	0.07(0.003)	0.01(0.002)
F	4.8(0.1)	4.92	4.6(0.2)	4.1(0.3)	4.9(0.1)	2.9(0.28)	1.7(0.31)	1.9(0.49)	1.7(0.18)	0.16(0.08)
Total	*100 (4.4)*	*98.0*	*97(6)*	*98(2)*	*98(1.5)*	*97.3(0.90)*	*96.0(0.48)*	*96.2(0.59)*	*96.4(1.38)*	*93.8(0.59)*
Mineral Formuals Calculated on the Basis of 11 Oxygens										
Si	2.528	2.704	2.598	2.584	2.532	2.822	2.778	2.754	2.767	3.424
Al	1.085	1.376	1.180	1.248	1.056	1.178	1.222	1.246	1.233	0.576
Al	-	-	-	-	-	0.050	0.047	0.026	0.002	0.675
Ti	0.192	0.134	0.166	0.187	0.184	0.209	0.205	0.226	0.199	0.003
Fe	1.923	1.661	1.921	2.062	2.023	1.043	1.125	1.155	1.115	1.319
Mn	0.139	0.202	0.169	0.186	0.132	0.039	0.039	0.036	0.040	0.003
Mg	0.806	0.241	0.535	0.336	0.743	1.529	1.485	1.469	1.561	0.485
Li						0.01	0.00	0.00	0.00	0.01
Rb	0.007	0.008	0.014	0.000	0.002	0.005	0.003	0.003	0.003	0.084
Ca	0.007	0.004	0.002	0.008	0.007	0.008	0.000	0.001	0.001	0.011
Na	0.084	0.102	0.082	0.069	0.067	0.061	0.059	0.062	0.060	0.012
K	0.804	0.870	0.824	0.835	0.836	0.881	0.898	0.874	0.925	0.803
Cl	0.029	0.074	0.043	0.031	0.027	0.011	0.009	0.010	0.009	0.002
F	0.582	0.590	0.574	0.513	0.600	0.345	0.211	0.238	0.210	0.019

Average major element analyses of trioctahedral micas from Thomas Range and Pine Grove. Numbers across the top represent grain numbers. N represents the number of analyses. Top values in wt% oxides, bottom are mineral formulas in apfu. The numbers in parentheses represent the standard deviation of the mean (1σ). Li calculated using data from LA-ICP-MS analyses of the same grains. BD stands for below detection. The dashes in the formula table for Al indicate that site assignment results have no Al in the tetrahedral site.

Table 9. Climax Major Element Trioctahedral Mica Analyses

	719r	721r				722r				723r					
	1(N=2)	1(N=2)	2(N=2)	3(N=2)	4(N=2)	1(N=2)	2(N=2)	3(N=2)	4(N=2)	1(N=2)	2(N=2)	3(N=2)	4(N=2)	5(N=2)	6(N=1)
SiO_2	38.6(0.02)	39.8(0.1)	34.6(4.68)	41.1(0.06)	39.6(0.26)	38.3(0.54)	38.0(0.53)	37.6(0.63)	38.3(0.55)	36.9(0.26)	36.4(0.29)	37.6(0.13)	37.5(0.11)	38.4(0.07)	37.45
Al_2O_3	17.5(0.39)	16.8(0.04)	15.7(1.01)	17.8(0.12)	16.6(0.21)	17.1(0.01)	19.0(0.25)	18.3(0.15)	19.1(0.29)	15.7(0.03)	17.4(0.07)	15.7(0.18)	15.7(0.15)	14.6(0.05)	15.77
TiO_2	1.2(0.01)	1.5(0.01)	1.5(0.02)	1.2(0.11)	1.3(0.07)	1.9(0.34)	1.2(0.05)	1.3(0.08)	1.2(0.06)	1.8(0.04)	1.8(0.01)	1.5(0.08)	2.2(0.64)	1.0(0.002)	1.80
FeO	14.2(0.08)	12.4(0.07)	12.6(0.20)	11.3(0.44)	11.9(0.03)	15.4(0.60)	15.3(0.06)	15.4(0.29)	15.3(.72)	16.1(0.37)	18.0(0.47)	16.3(0.09)	16.1(0.15)	13.7(0.20)	16.47
MnO	2.4(0.2)	1.3(0.04)	1.3(0.08)	1.6(0.07)	1.4(0.04)	3.0(0.12)	2.9(0.08)	2.8(0.02)	2.9(0.07)	0.7(0.02)	0.48(0.02)	0.44(0.06)	0.47(0.03)	0.47(0.01)	0.41
MgO	8.9(0.48)	10.7(0.05)	10.9(0.10)	8.9(0.05)	10.7(0.11)	7.6(0.36)	4.7(0.02)	6.7(0.01)	4.9(0.16)	12.0(0.02)	10.8(0.19)	12.6(0.30)	12.5(0.06)	14.5(0.06)	11.75
Li_2O	N/A	0.76(0.11)	0.73(0.08)	0.12(0.005)	0.76(0.17)	0.44(0.24)	0.18(0.05)	0.24(0.003)	0.35(0.12)	0.18(0.03)	N/A	0.11(0.02)	0.08(0.003)	0.26(0.07)	0.07
Rb_2O	0.9(0.01)	0.49(0.03)	0.62(0.14)	0.72(0.01)	0.61(0.08)	0.28(0.19)	1.2(0.17)	1.1(0.14)	1.4(0.03)	0.39(0.03)	0.44(0.07)	0.51(0.04)	0.39(0.04)	0.46(0.05)	0.40
CaO	BD	BD	BD	0.01(0.005)	0.01(0.004)	BD	0.05(0.02)	0.001(0.0009)	0.01(0.005)	0.001(0.000)	0.01(0.005)	BD	BD	0.01(0.01)	0.003
Na_2O	0.17(0.03)	0.19(0.01)	0.17(0.02)	0.19(0.03)	0.23(0.01)	0.26(0.01)	0.14(0.01)	0.17(0.02)	0.18(0.01)	0.04(0.03)	0.12(0.003)	0.16(0.02)	0.08(0.01)	0.10(0.003)	0.15
K_2O	9.9(0.11)	10.0(0.06)	9.9(0.22)	10.1(0.05)	10.1(0.08)	9.9(0.09)	9.7(0.11)	9.7(0.03)	9.8(0.05)	9.8(0.003)	9.9(0.02)	9.8(0.03)	9.8(0.02)	10.1(0.04)	10.03
Cl	0.02(0.0003)	0.03(0.001)	0.03(0.002)	0.02(0.002)	0.03(0.01)	0.040(0.01)	0.05(0.02)	0.04(0.01)	0.04(0.01)	0.06(0.003)	0.11(0.02)	0.09(0.004)	0.08(0.01)	0.05(0.01)	0.11
F	1.7(0.7)	2.6(0.41)	2.7(0.06)	2.8(0.07)	2.6(0.01)	1.0(0.52)	BD	0.31(0.14)	0.53(0.32)	BD	BD	BD	BD	0.76(0.09)	BD
Total	*95.5(0.44)*	*95.9(0.12)*	*90.1(5.9)*	*95.7(0.89)*	*95.1(0.43)*	*94.4(0.41)*	*92.4(0.76)*	*93.3(0.79)*	*93.7(0.41)*	*93.6(0.62)*	95.4(0.01)	94.8(0.41)	94.8(0.55)	94.2(0.21)	94.34
Mineral Formuals Calculated on the Basis of 11 Oxygens															
Si	2.947	2.971	2.818	3.083	2.987	2.927	2.968	2.916	2.956	2.841	2.774	2.857	2.843	2.916	2.862
Al	1.053	1.029	1.182	0.917	1.013	1.073	1.032	1.084	1.044	1.159	1.226	1.143	1.157	1.084	1.138
Al	0.523	0.451	0.319	0.657	0.459	0.466	0.719	0.583	0.698	0.261	0.334	0.262	0.246	0.225	0.282
Ti	0.070	0.087	0.093	0.070	0.072	0.108	0.071	0.078	0.067	0.103	0.103	0.088	0.124	0.058	0.103
Fe	0.907	0.773	0.854	0.708	0.751	0.985	1.000	0.997	0.986	1.035	1.147	1.036	1.021	0.873	1.052
Mn	0.159	0.085	0.090	0.100	0.091	0.196	0.195	0.183	0.193	0.047	0.031	0.028	0.030	0.030	0.027
Mg	1.021	1.191	1.322	0.992	1.203	0.862	0.545	0.777	0.573	1.378	1.224	1.422	1.408	1.638	1.338
Li	0.000	0.228	0.239	0.038	0.230	0.134	0.057	0.074	0.109	0.057	0.000	0.033	0.025	0.078	0.023
Rb	0.042	0.023	0.032	0.035	0.030	0.014	0.061	0.053	0.068	0.019	0.021	0.025	0.019	0.023	0.020
Ca	0.000	0.000	0.000	0.000	0.001	0.000	0.004	0.000	0.000	0.000	0.000	0.000	0.000	0.001	0.000
Na	0.025	0.028	0.026	0.028	0.033	0.038	0.021	0.026	0.028	0.006	0.017	0.023	0.012	0.016	0.022
K	0.962	0.952	1.025	0.968	0.966	0.972	0.964	0.959	0.968	0.963	0.965	0.952	0.947	0.977	0.978
Cl	0.003	0.004	0.004	0.003	0.003	0.005	0.007	0.005	0.006	0.008	0.014	0.012	0.010	0.006	0.014
F	0.199	0.306	0.349	0.333	0.313	0.088	0.000	0.038	0.064	0.000	0.000	0.000	0.000	0.092	0.000

Average major element analyses of trioctahedral micas from Climax. Numbers across the top represent grain numbers. N represents the number of analyses. Top values in wt% oxides, bottom are mineral formulas in apfu. The numbers in parentheses represent the standard deviation of the mean (1σ). Li calculated using data from LA-ICP-MS analyses of the same grains expect for those labeled with N/A. BD stands for below detection.

LA-ICP-MS analyses were successfully completed for phases of interest in thin sections from Mount Pleasant, the topaz-rhyolites from Thomas Range and Pine Grove, and Climax. Trioctahedral micas were analyzed for trace element data in Mount Pleasant sample MP-91-1.36, Thomas Range samples 109593-10 and 109593-13, and Climax samples 721r, 722r, and 723r (Table 10). Pine Grove sample Pine 7 Tbpa contained other sheet silicates (such as chlorite) and some amphibole analyses that are reported in appendix Table B.3. Muscovite were analyzed in Pine Grove sample Pine 2 Tpg and are reported in appendix Table B.3.

Table 10. Trace Element Analyses of Trioctahedral Micas

	Mount Pleasant	Thomas Range (109593-10)			Thomas Range (109593-13)
	(N=15)	Type 1 (N=8)	Type 2 (N=2)	Type 3 (N=1)	(N=11)
^{6}Li	12100(300)	410(22)	1590(54)	2579	50.6(9.7)
^{7}Li	13500(300)	400(20)	1700(67)	2736	BD
^{9}Be	30(1)	5.3(0.3)	3.9(0.3)	2.61	0.67(0.10)
^{45}Sc	25.3(0.92)	24(2.6)	62(2)	72.8	32.1(1.2)
^{53}Cr	BD	BD	BD	BD	12.33
^{67}Zn	447(9)	600(17)	760(25)	835	1970.18
^{69}Ga	53(2.5)	39(4.8)	48(7.6)	40.7	869.33
^{85}Rb	8400(180)	724(8.1)	875(2.5)	2391	512.79
^{88}Sr	1(0.3)	6(1.8)	8(4.8)	1.39	8.20
^{89}Y	3(2)	1.5(0.1)	3.2(0.45)	0.85	0.66
^{90}Zr	0.40(0.07)	4.6(0.2)	7.4(0.4)	11.6	4.05
^{93}Nb	220(20)	192(2.5)	286(12.5)	1223	71.51
^{97}Mo	0.45(0.03)	1.9(0.15)	5(1.1)	25.4	0.40
^{111}Cd	0.10(0.03)	0.2(0.06)	0.1	0	0.08
^{115}In	0.94(0.04)	0.28(0.04)	0.27(0.02)	0.27	0.22
^{118}Sn	160(12)	4(0.5)	4.7(0.44)	7.22	6.86
^{133}Cs	480(53)	11(0.3)	10.3(1.2)	52.1	10.30
$_{139}$La	0.10(0.01)	1.2(0.2)	3.3(0.6)	1.36	0.41
^{140}Ce	0.08(0.03)	6(0.5)	16(3.6)	19.4	1.15
^{141}Pr	0.04(0.006)	0.38(0.04)	1.3(0.4)	0.37	0.16
^{146}Nd	0.03(0.01)	1.1(0.15)	3.4(0.9)	0.99	0.53
^{147}Sm	0.03(0.007)	0.3(0.02)	0.66(0.05)	0.06	0.10
^{151}Eu	BD	0.01(0.002)	BD	0.02	0.52
^{157}Gd	0.05(0.02)	0.24(0.03)	0.5	0.10	0.15
^{159}Tb	0.02(0.01)	0.05(0.01)	0.1(0.02)	0.06	0.01
^{163}Dy	0.3(0.2)	0.3(0.03)	0.55(0.02)	0.12	0.09
^{165}Ho	0.08(0.07)	0.08(0.01)	0.11(0.01)	0.02	0.01
^{166}Er	0.4(0.36)	0.27(0.03)	0.48(0.07)	0.18	0.02
^{169}Tm	0.07(0.06)	0.05(0.01)	0.09(0.01)	0.06	0.00
^{172}Yb	0.5(0.4)	0.45(0.04)	0.51(0.02)	0.25	0.04
^{175}Lu	0.1(0.07)	0.07(0.01)	0.09(0.01)	0.02	0.01
^{178}Hf	0.05(0.01)	0.16(0.02)	0.44(0.08)	0.98	0.20
^{181}Ta	38(6)	3.4(0.07)	7(1.1)	76.5	1.36
^{183}W	21(0.9)	2.8(0.3)	2.3(0.6)	12.0	0.21
^{232}Th	0.07(0.01)	12(1.9)	6.5(0.32)	13.9	0.27
^{238}U	0.13(0.04)	1(0.1)	1.8(0.34)	1.66	0.07

Average trace element analyses of trioctahedral micas from Mount Pleasant, Utah, and Climax. represents the number of analyses. Values in ppm. The numbers in parentheses represent the standard deviation of the mean (1σ). BD means below detection.

Table 10. Element Analyses of Trioctahedral Micas continued

	Climax (721r)	Climax (722r)	Climax (723r)
	(N=10)	(N=11)	(N=10)
^{6}Li	3645(322)	1472(380)	690(188)
^{7}Li	4147(332)	987(421)	716(78.3)
^{9}Be	7.5(1.9)	7.8(1.5)	2.4(0.45)
^{45}Sc	106(9.2)	389(23.1)	33.6(4.2)
^{53}Cr	80.7(10.3)	4.5	24.2(1.7)
^{67}Zn	603(39.4)	1052(145)	454(25.9)
^{69}Ga	131(13.8)	125(30.5)	102(16.7)
^{85}Rb	3095(153)	4176(551)	1629(247)
^{88}Sr	1.9(0.18)	1.2(0.39)	6.4(1.1)
^{89}Y	0.04(0.008)	0.71(0.31)	1.3(0.7)
^{90}Zr	1.0(0.36)	1.3(0.51)	2.6(0.94)
^{93}Nb	35.7(8.6)	162(11.5)	69.6(38.5)
^{97}Mo	0.31(0.12)	0.23(0.01)	0.32(0.13)
^{111}Cd	0.36(0.08)	0.35(0.05)	BD
^{115}In	0.50(0.05)	1.7(0.17)	0.54(0.09)
^{118}Sn	95.0(7.6)	276(43.6)	72.8(15.0)
^{133}Cs	22.4(1.5)	43.4(7.8)	13.0(7.3)
$_{139}$La	0.01(0.006)	0.18(0.05)	0.67(0.35)
^{140}Ce	0.006(0.004)	0.41(0.13)	1.5(0.64)
^{141}Pr	0.003(0.002)	0.08(0.02)	0.22(0.07)
^{146}Nd	0.006(0.006)	0.24(0.09)	0.57(0.29)
^{147}Sm	0.01(0.009)	0.11(0.04)	0.10(0.05)
^{151}Eu	0.01(0.005)	0.02(0.006)	0.07(0.02)
^{157}Gd	0.04(0.02)	0.12(0.04)	0.18(0.08)
^{159}Tb	0.001(0.0007)	0.02(0.009)	0.03(0.02)
^{163}Dy	0.01(0.008)	0.08(0.04)	0.28(0.14)
^{165}Ho	0.002(0.001)	0.03(0.02)	0.06(0.04)
^{166}Er	0.001(0.001)	0.06(0.03)	0.17(0.08)
^{169}Tm	0.003104473	0.02(0.007)	0.02(0.02)
^{172}Yb	0.003(0.003)	0.12(0.06)	0.11(0.05)
^{175}Lu	0.003(0.001)	0.02(0.006)	0.03(0.02)
^{178}Hf	0.07(0.006)	0.22(0.06)	0.12(0.05)
^{181}Ta	1.6(0.47)	12.9(3..2)	3.2(1.1)
^{183}W	1.5(0.27)	6.3(1.9)	33.3(15.9)
^{232}Th	0.002(0.001)	0.29(0.13)	0.40(0.15)
^{238}U	0.12(0.007)	1.7(0.45)	0.62(0.33)

Discussion

Tischendorf (2007) explored mica compositions and solid solution series and came up with a method of plotting various mica endmembers on the same diagram based on the

occupancy of the octahedral site. The y-axis is feal, which is the atoms per formula unit of Fe, Mn, and Ti in the octahedral site subtracted by the aluminum content in the octahedral site. The x-axis is mgli, which is the magnesium content subtracted by the lithium content in the octahedral site. All mica compositions from Mount Pleasant, the topaz-rhyolites of Utah, and Climax are plotted on the diagram of Tischendorf (Figure 9). The Thomas Range Crystal Tuff Member is scattered roughly along the annite-phlogopite (biotite) solid solution line, closer to the annite side. Some of the Thomas Range Crystal Tuff Member points plot outside of the realm of known compositions: this is likely due to the presence of Fe^{3+} in the tetrahedral site, which cannot be measured on the probe, and an estimation of the Fe^{3+} content would bring the compositions back to the solid solution line. Mount Pleasant has a relatively low spread is between polylithionite and siderophyllite. The Thomas Range Alkali Rhyolite and Vitrophyre points are also well constrained and plot close to the center on the annite-phlogopite solid solution line. Pine Grove and Climax plot in the center right.

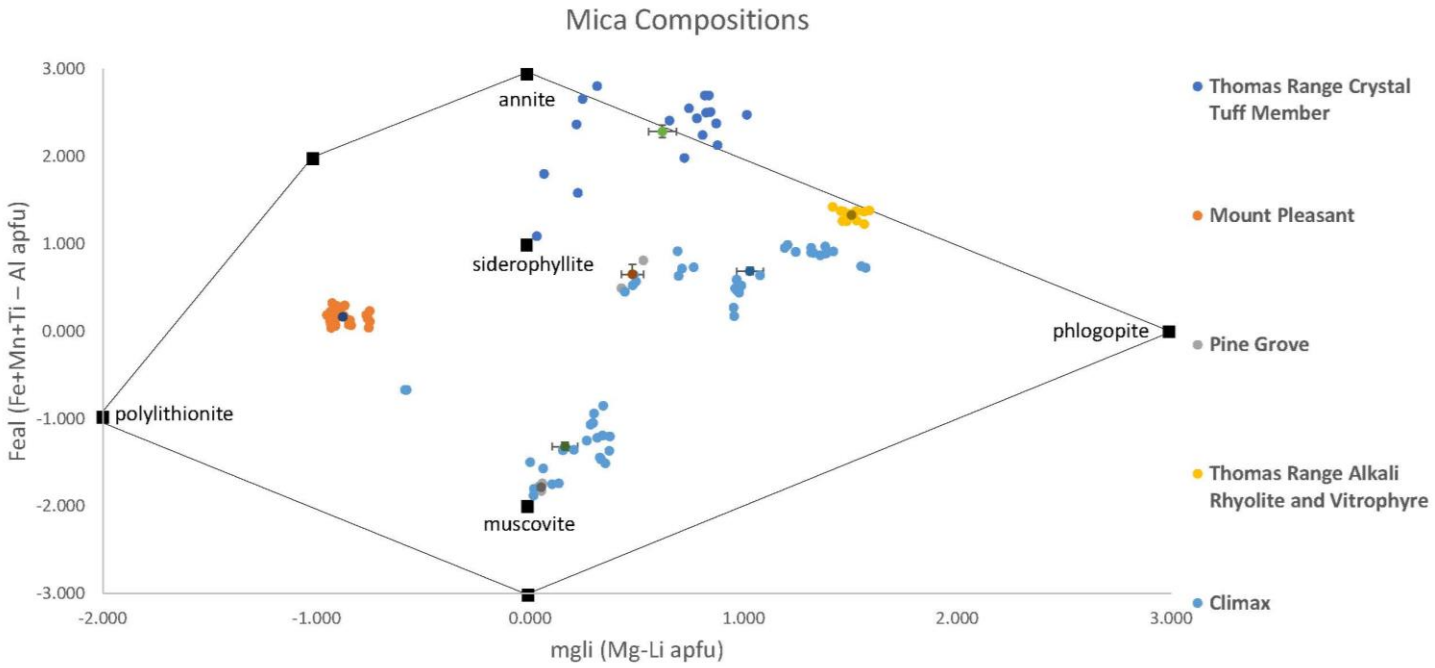

Figure 9. Mica Compositions described in a two-dimensional plot according to the occupancy of the octahedral site. The x-axis is Mgli = Mg – Li and the y-axis is feal = Fe+Mn+Ti – Al after Tischendorf et al., 2004. Black lines represent solid solution between the end members and are the bounds of known mica compositions. Uncertainty in a single point is due to counting statistics. The mean of each population is plotted with error bars that represent the standard deviation of the mean.

For the Climax Li data taken on October 30, 2019 the instrument had lower sensitivity with each subsequent block of analyses to down to approximately 1/20 of what it was at the start of the day. These data have been included here for completion sake only and may have higher lithium content. This could account for why there is a large horizontal spread, since lithium is a part of the x-axis, but the spread along the y-axis is minimal.

To examine compositional differences between just the trioctahedral micas, X_{Ann}^{Bt}(or X_{annite}), the proportion of iron in the octahedral site, is plotted versus the total aluminum in both the tetrahedral and octahedral sites (Figure 10). The three topaz-rhyolite populations, Thomas Range Crystal Tuff Member, Pine Grove, and Thomas Range Alkali Rhyolite and Vitrophyre, have differing X_{annite} proportions but all plot similarly in regard to total aluminum. Climax and Mount Pleasant have differing aluminum contents but similar X_{annite}. The topaz-rhyolite unit Thomas Range Alkali Rhyolite and Vitrophyre also has similar X_{annite} ti that of Mount Pleasant and Climax, though Climax is closer to Mount Pleasant.

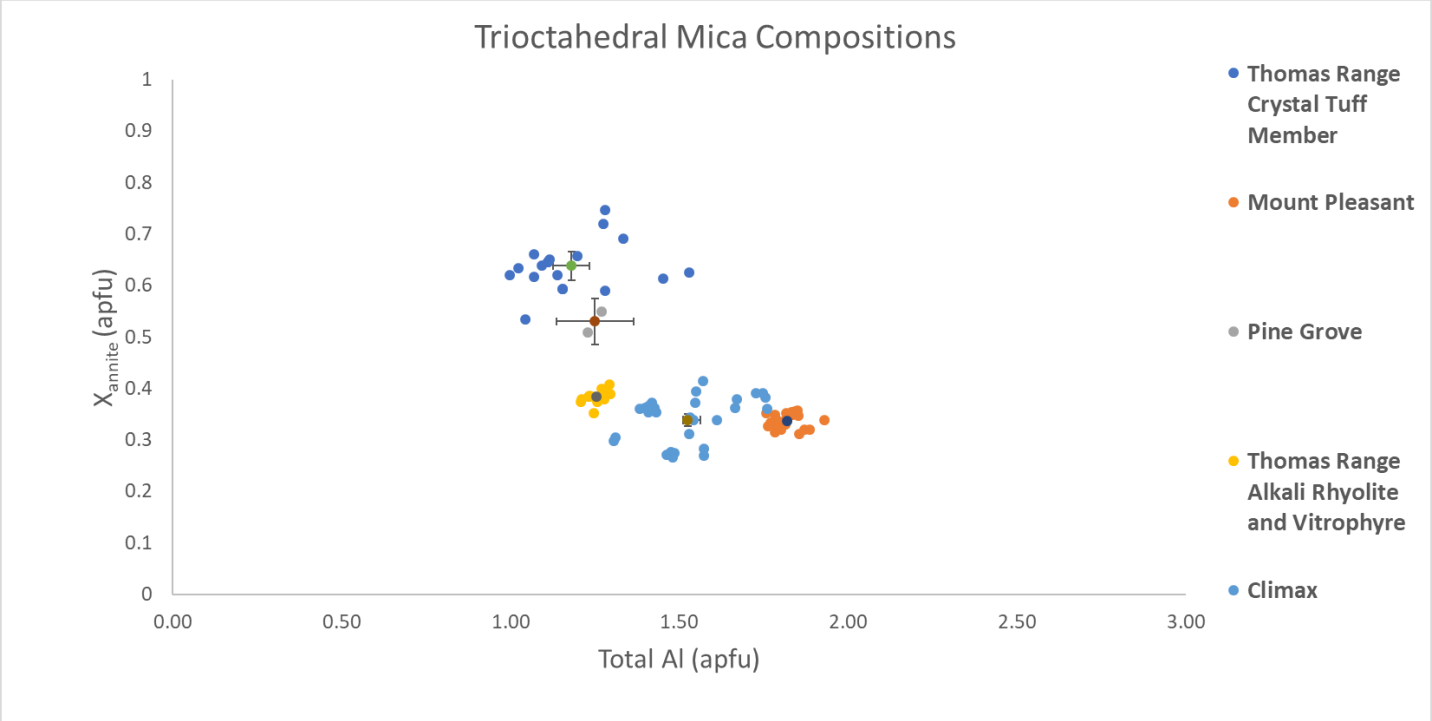

Figure 10. Trioctahedral mica compositions plotted as X_{annite} (X_{Ann}^{Bt}) vs Total Al. The x-axis is X_{annite} = Fe / (Al+Ti+Fe+Mn+Mg+Li) in the octahedral site. The y-axis is total Al from the tetrahedral and octahedral sites. Uncertainty in a single point is due to counting statistics. The mean of each population is plotted with error bars that represent the standard deviation of the mean.

Two of the discriminatory elements between A-types and topaz-rhyolites are lithium and rubidium (Table 4 and Christiansen 1983). Due to their importance and the amounts of them found in some of the samples, lithium was plotted vs rubidium in trioctahedral micas (Figure 11). Mount Pleasant is highly enriched in both lithium and rubidium, while all of the topaz-rhyolites are relatively depleted in both with the exception of some of the Thomas Range Crystal Tuff Member grains which have appreciable, but still minor amounts. Climax plots in between the topaz-rhyolites and Mount Pleasant, however, similar to the lithium in Figure 9, regarding the Climax lithium data taken on October 30, 2019, the instrument had lower sensitivity with each subsequent block of analyses to down to approximately 1/20 of what it was at the start of the day. The actual lithium content is likely less and could account for the large spread in the data. There appears to be trend of increasing rubidium and lithium from the topaz-rhyolites, to Climax,

to Mount Pleasant. Whether this a real trend due to a geologic process such as fractionation or merely circumstantial is unknown.

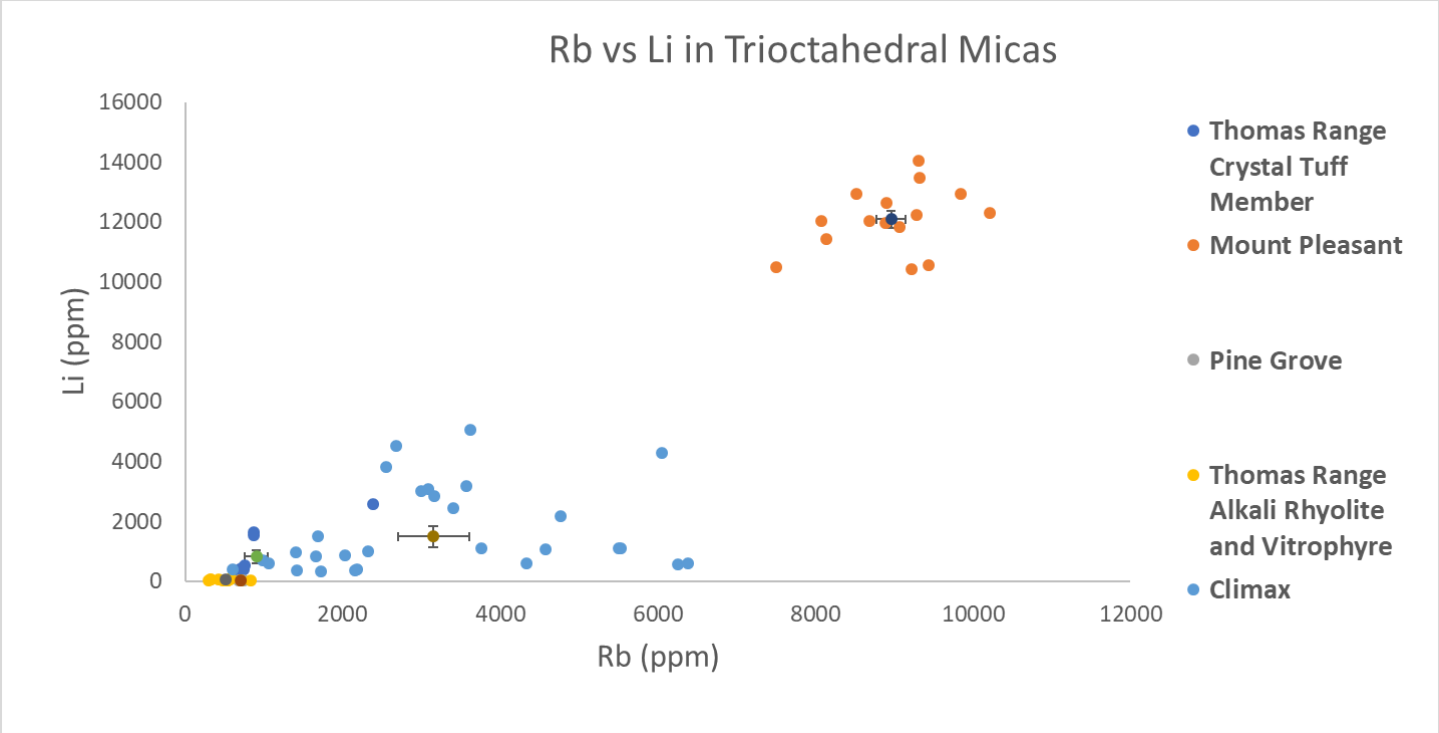

Figure 11. Rb and Li contents in trioctahedral micas. Uncertainty in a single point is due to counting statistics. The mean of each population is plotted with error bars that represent the standard deviation of the mean.

To quantitively test the hypotheses, t-tests were performed to compare the distinguishing

Table 11. Statistical Analyses

Variable	Mount Pleasant vs Topaz-rhyolites	Mount Pleasant vs Climax	Topaz-rhyolites vs Climax
Li			
Rb			
X_{Ann}^{Bt}			
Zr			
La			
Lu			

Results of T tests performed between the trioctahedral micas from Mount Pleasant, the topaz-rhyolites of Utah, and Climax. Green means that they were statistically indistinguishable from each other at the 0.05 level of significance. Red means the they are statistically different at the 0.05 level of significance. Yellow means that the T test shows that they are statistically distinguishable at the 0.05 level but statistically indistinguishable at the 0.047 level.

variables between A-type and topaz-rhyolites from Table 5 in addition to others of possible interest (Table 11). The elements Li, Rb, and Zr were chosen because they are several of the discriminatory trace elements between the types of magmatism (Table 4 and Christiansen 1983). Another one of the discriminatory characteristics is the REE content (Table 4 and Christiansen

1983). Lanthanum is being used as a proxy to represent LREEs, and lutetium as a proxy to represent the HREEs. X_{Ann}^{Bt} is the proportion of iron in the octahedral site and can be used to compare mica compositions so it was included to get a sense of compositional comparisons between the sites. Lutetium is statistically similar between all the sites, which would make sense since both A-type and topaz-rhyolites are enriched in HREEs, such as lutetium. Other than lutetium, Mount Pleasant trioctahedral micas are statistically different from the topaz-rhyolite trioctahedral micas in every variable. Mount Pleasant trioctahedral micas are statistically different from Climax trioctahedral micas in Li, Rb, and Zr, and similar in X_{Ann}^{Bt}. Although the trioctahedral micas from Mount Pleasant and Climax are statistically different for lanthanum at the 0.05 level, they are indistinguishable at the 0.047 level, which is very close. Besides lutetium, the only other variable that is similar between the trioctahedral micas from the topaz-rhyolites and Climax is lithium, with all others being statistically different. Each of the t-tests has its own null hypothesis that there is no difference in the variable being tested in the trioctahedral micas in the rocks from Mt. Pleasant, Climax, and the topaz-rhyolites of Utah. The null hypotheses for Mount Pleasant vs the topaz-rhyolites were disproven for all the variables except lutetium. The null hypotheses for Mount Pleasant vs Climax were disproven for Li, Rb, Zr, and La (though only by a small margin for La) and not for X_{Ann}^{Bt}. The null hypotheses for the topaz-rhyolites vs Climax were disproven for Rb, X_{Ann}^{Bt}, Zr, and La and not for lithium and lutetium. Given the results of the tests, the type of magmatism that formed Mount Pleasant cannot be determined to be A-type or topaz-rhyolite, however, it appears to be closer to Climax (A-type).

Conclusions and Broader Impacts

Although the type of magmatism that formed Mount Pleasant cannot be definitively constrained as A-type or topaz-rhyolite based on statistical comparisons of key variables between the sample sites, Mount Pleasant appears to be closer in relation to the Climax A-types. Other than lutetium, which is statistically indistinguishable at the 0.05 level of significance between all the sites, only Climax showed additional similarities to Mount Pleasant (Table 11). This includes the X_{Ann}^{Bt}, and while not actually statistically different, the lanthanum content was very close to being similar (at the 0.05 level it's different but it is statistically indistinguishable at the 0.047 level). Mount Pleasant also plots closest to Climax in both Figure 10 and Figure 11. Despite these similarities, there are still several key variables that remain different between Mount Pleasant and Climax (Figure 9 and Table 11).

A potential reason for this lack of a clear classification is that all of the sites represent different parts of the same genetic family. Future work to investigate this could include additional analyses of the sample sites looked at in this study in addition to adding new sites of the relevant types and examining the whole rock data related to them. This research could lead to insights into how A-type and topaz-rhyolite magmatism are related, and potentially a correlation between magma type and ore deposit type.

Acknowledgements

A variety of organizations and individuals gave support to this project. The late Dr. James Webster, former curator at the American Museum of Natural History, kindly provided the samples of Mount Pleasant. Samples of topaz-rhyolites were provided by Leslie Hale at the

National Museum of Natural History at the Smithsonian Institution and Dr. Andreas Audétat at the Bayerisches Geoinstitut Universität Bayreuth, Germany. James Hagadorn at The Denver Museum of Nature and Science provided the samples from Climax. This work is supported by the NSF grant #1348010.

Bibliography

Adex Mining Inc. (2014). http://www.adexmining.com/. Accessed April 5, 2019.

Audétat, A., Li, W. (2017). The genesis of Climax-type porphyry Mo deposits: Insights from fluid inclusions and melt inclusions. *Ore Geology Reviews* 88,436-460.

Abdel-Rahman, A.M. (1994). Nature of Biotites from Alkaline, Calc-alkaline, and Peraluminous Magmas. *Journal of Petrology* 35:2,525-541.

Chappell, B.W., and White, A.J.R. (1974). Two Contrasting Granite Types. *Pacific Geology* 8,173-174.

Christiansen, E.H., et al. (1983). The Petrogenesis of Topaz Rhyolites from the Western United States. *Contributions to Mineralogy and Petrology* 83,16-30.

Christiansen, E.H., Sheridan, M.F., and Burt, D.M. (1986). The Geology and Geochemistry of Cenozoic Topaz Rhyolites from the Western United States. *Geological Society of America Special Paper* 205.

Clemens, J.D., Holloway, J.R., and White, A.J.R (1986). Origin of an A-type Granite: Experimental Constraints. *American Mineralogist* 71,317-324.

Climax Molybdenum Company (2013). http://www.climaxmolybdenum.com/index.htm. Accessed April 5, 2019.

Hedenquist, J.W., and Lowenstern, J.B. (1994). The Role of Magmas in the Formation of Hydrothermal Ore Deposits. *Nature* 370, 519-527.

Inverno, C.M.C., and Hutchinson, R.W. (2006). Petrochemical Discrimination of Evolved Granitic Intrusions Associated with Mount Pleasant Deposits, New Brunswick, Canada. *Applied Earth Science* 115:1,23-39.

Jackson, S. (2008). LAMTRACE data reduction software for LA-ICP-MS. *Laser Ablation ICP-MS in the Earth Sciences: Current Practices and Outstanding Issues* 40.

Loiselle, M.C., and Wones, D.R. (1979). Characteristics and Origin of Anorogenic Granites. *Geological Society of America, Abstracts with Programs* 11,468.

Nesse, W.D. (2016) *Introduction to Mineralogy 3rd Edition*. Oxford University Press.

Shabani, A., et al. (2003). Composition of Biotite from Granitic rocks of the Canadian Appalachian Orogen: A Potential Tectonomagamtic Indicator. *The Canadian Mineralogist* 41:6,1381-1396.

Sinclair, W.D., et al. (2006). Geology, Geochemistry and Mineralogy of Indium Resources at Mount Pleasant, New Brunswick, Canada. *Ore Geology Reviews* 28,123-145.

Sinclair, W.D., Kooiman, G.J.A., and Taylor R.P. (2007). Petrochemical Discrimination of Evolved Granitic Intrusions Associated with Mount Pleasant Deposits, New Brunswick, Canada by Inverno, C.M.C., and Hutchinson R.W. *Applied Earth Science* 116:2,106-111.

Staatz, M.H., and Carr, W.J. (1964). Geology and Mineral Deposits of the Thomas and Dugway Ranges Juab and Tooele Counties Utah. *USGS Professional Paper 415* 188p.

Tischendorf, G., et al. (2007). True and Brittle Micas: Composition and solid-solution series. *Mineralogical Magazine* 71:3,285-320

U.S. Geological Survey (2018). Mineral Commodity Summaries 2018. *U.S. Geological Survey* 200p.

Wallace, S.R. (1995). The Climax-type Molybdenite Deposits: What they are, Where they are, and Why they are. *Economic Geology* 90,1359-1380

Wallace, S.R., et al. (1968). Multiple Intrusion and Mineralization at Climax, Colorado, in Ridge, J.D. 1968. *Ore Deposits in the United States* 1933-1967,605-640

Appendices

Appendix A: EPMA Analyses

Table A.1: EPMA analyses of trioctahedral micas from Mount Pleasant and Thomas Range

No.	Na_2O	K2O	CaO	FeO	F	Rb_2O	Cl	TiO_2	MnO	SiO_2	MgO	Al_2O_3	Total	Comment
1	0.56	8.7	0.119	27.6	4.9	0.2	0.2	3.2	1.8	35.3	7.7	12.5	100.8	Thomas Range Biotite 1.1
2	0.55	8.4	0.061	29.9	5.1	0.1	0.2	3.2	2.1	33.3	7.4	11.1	99.2	Thomas Range Biotite 1.2
3	0.63	9.0	0.064	25.7	5.1	0.2	0.3	3.3	2.2	35.1	6.3	13.7	99.3	Thomas Range Biotite 1.3
4	0.53	7.6	0.091	33.8	4.5	0.2	0.2	3.5	2.4	31.1	7.1	11.5	100.5	Thomas Range Biotite 1.4
5	0.56	7.6	0.072	33.8	4.6	0.1	0.2	3.5	2.3	31.1	6.9	11.5	100.2	Thomas Range Biotite 1.5
6	0.10	0.9	0.183	3.0	1.0	0.2	0.1	0.2	0.4	87.2	0.3	2.2	95.3	Thomas Range Biotite 2.1
7	0.69	9.0	0.049	26.2	4.9	0.2	0.6	2.3	3.1	35.6	2.1	15.4	98.0	Thomas Range Biotite 2.2
8	1.14	4.1	0.074	7.4	1.6	0.3	0.2	0.5	1.1	73.5	0.5	7.6	97.3	Thomas Range Biotite 2.3
9	0.46	7.6	0.037	21.9	4.4	0.3	0.5	1.7	2.6	46.9	1.9	11.9	BD	Thomas Range Biotite 2.4
10	0.64	8.6	0.087	29.6	4.5	0.2	0.2	3.1	BD	30.9	6.6	10.0	94.6	Thomas Range Biotite 3.1
11	0.61	8.6	BD	25.6	4.9	0.6	0.6	1.6	3.1	36.4	2.1	16.2	98.2	Thomas Range Biotite 3.2
12	0.35	5.8	0.032	24.8	2.9	0.3	0.3	2.1	1.1	25.2	6.6	8.0	76.2	Thomas Range Biotite 3.3
13	0.50	8.1	0.036	28.5	4.8	0.1	0.2	2.9	2.1	34.4	6.9	12.0	98.5	Thomas Range Biotite 3.4
14	0.42	7.8	0.008	33.9	4.3	0.2	0.3	3.7	2.9	31.3	2.7	13.0	98.5	Thomas Range Biotite 3.5
15	0.44	8.2	0.081	32.8	3.9	0.1	0.2	3.2	2.8	32.4	3.0	13.1	98.6	Thomas Range Biotite 4.1
16	0.46	8.5	0.110	30.1	4.4	BD	0.2	3.1	2.8	33.6	2.8	13.9	98.1	Thomas Range Biotite 4.2
17	0.43	8.5	BD	32.0	5.2	0.1	0.2	3.2	2.0	32.5	6.3	11.0	99.1	Thomas Range Biotite 5.1
18	0.40	8.3	0.045	29.5	4.7	0.1	0.2	3.1	2.3	32.5	5.5	12.2	96.8	Thomas Range Biotite 5.2
19	0.46	8.5	0.008	32.0	5.0	0.1	0.2	3.2	1.9	32.3	7.2	11.4	100.0	Thomas Range Biotite 5.3
20	0.48	8.3	0.316	30.7	4.6	0.0	0.2	3.1	1.8	32.7	6.6	11.5	98.5	Thomas Range Biotite 5.4
21	0.29	10.1	0.028	15.2	5.6	2.2	0.01	0.21	1.4	42.8	0.1	20.3	95.8	MP-91-1.36 Biotite 1.1
22	0.19	10.1	0.007	16.7	5.4	2.0	0.02	0.43	1.3	41.4	0.0	20.9	96.3	MP-91-1.36 Biotite 1.2
23	0.27	10.0	0.011	15.8	5.5	1.8	0.00	0.38	1.6	41.9	0.0	20.4	95.5	MP-91-1.36 Biotite 1.3
24	0.20	10.4	BD	16.8	5.3	2.0	0.02	0.80	1.2	42.5	0.0	20.5	97.6	MP-91-1.36 Biotite 1.4
25	0.17	10.3	BD	16.1	4.7	1.6	0.01	0.23	1.4	42.2	0.0	21.0	95.6	MP-91-1.36 Biotite 1.5
26	0.21	9.9	BD	14.3	5.3	1.9	0.01	0.25	1.3	42.0	0.1	20.2	93.3	MP-91-1.36 Biotite 2.1
27	0.27	9.6	0.021	14.8	5.2	1.9	0.01	0.11	1.4	41.1	0.1	21.2	93.5	MP-91-1.36 Biotite 2.2
28	0.36	9.4	BD	15.4	6.1	2.0	0.02	0.05	1.4	38.2	0.0	21.0	91.4	MP-91-1.36 Biotite 2.3
29	0.10	10.2	BD	14.1	6.1	2.0	BD	0.12	1.4	40.7	0.0	20.7	92.8	MP-91-1.36 Biotite 2.4
30	0.29	9.7	BD	14.5	6.0	2.0	0.01	0.29	1.4	39.2	0.1	20.7	91.6	MP-91-1.36 Biotite 2.5
31	0.12	10.2	0.030	16.1	4.9	1.9	0.01	0.44	1.3	41.9	0.1	21.0	96.0	MP-91-1.36 Biotite 3.1
32	0.14	10.2	0.013	15.3	4.8	2.0	0.00	0.60	1.5	40.9	0.1	20.2	93.7	MP-91-1.36 Biotite 3.2
33	0.19	10.1	BD	14.8	5.3	1.9	0.01	0.44	1.1	41.9	0.0	20.5	94.0	MP-91-1.36 Biotite 3.3

34	0.18	10.1	0.004	16.5	4.5	1.9	0.01	0.60	1.7	41.2	0.0	20.3	95.1	MP-91-1.36 Biotite 3.4
35	0.30	10.0	0.035	16.4	5.3	1.6	0.02	0.23	1.6	41.6	0.0	20.9	95.7	MP-91-1.36 Biotite 3.5
36	0.26	9.6	BD	14.6	5.6	2.2	0.01	0.15	1.5	42.6	0.0	20.2	94.3	MP-91-1.36 Biotite 4.1
37	0.24	9.8	BD	15.7	5.2	1.7	0.01	0.32	1.4	41.3	0.0	20.6	94.2	MP-91-1.36 Biotite 4.2
38	0.28	9.7	BD	15.6	5.5	1.8	0.03	0.23	1.4	41.6	0.1	21.0	94.9	MP-91-1.36 Biotite 4.3
39	0.38	9.4	BD	16.2	5.2	2.0	0.02	0.59	1.7	BD	0.0	21.1	95.6	MP-91-1.36 Biotite 4.4
40	0.20	9.7	0.037	15.7	4.5	1.8	0.09	0.41	1.4	40.6	0.0	20.5	93.1	MP-91-1.36 Biotite 4.5
41	0.22	10.0	BD	15.2	5.9	2.2	0.01	0.29	1.4	42.5	0.0	20.2	95.5	MP-91-1.36 Biotite 5.1
42	0.24	9.9	0.016	14.6	5.6	2.3	BD	0.28	1.4	42.1	0.0	20.4	94.6	MP-91-1.36 Biotite 5.2
43	0.31	9.8	BD	16.3	5.7	1.8	0.01	0.26	1.8	39.7	0.0	20.5	93.7	MP-91-1.36 Biotite 5.3
44	0.25	9.9	0.002	15.1	5.7	2.1	0.01	0.20	1.5	40.5	0.0	19.7	92.7	MP-91-1.36 Biotite 5.4
45	0.3	9.8	0.0	15.6	5.3	1.6	0.02	0.14	1.4	39.5	0.0	20.0	91.4	MP-91-1.36 Biotite 5.5
46	0.3	10.1	0.0	15.1	5.8	2.1	0.01	0.14	1.4	42.6	0.0	20.9	96.0	MP-91-1.36 Biotite 5.6

Trioctahedral mica analyses performed via EPMA. BD represents values that were below the detection limit of the instrument. In wt% oxide. Text in red denotes anomalous analyses (low total): they were not used in subsequent calculations.

Table A.2: EPMA analyses of fluorite from Mount Pleasant

No.	Na	Cl	Ca	Fe	F	Mg	Mn	Al	Total	Comment
1	BD	BD	53.7	BD	45.4	0.010	0	0.28	99.4	MP-91-1.19 Fluorite 1.1
2	0.001	0.001	52.7	BD	47.0	BD	BD	0.001	99.6	MP-91-1.19 Fluorite 1.2
3	0.01	0.004	52.8	0.10	46.6	0.002	0.009	BD	99.5	MP-91-1.19 Fluorite 1.3
4	BD	0.006	52.5	0.01	45.7	BD	BD	BD	98.2	MP-91-1.19 Fluorite 1.4
5	BD	0	52.4	BD	46.2	BD	0.11	0.02	98.7	MP-91-1.19 Fluorite 1.5
6	BD	BD	54.2	0.002	47.0	BD	BD	0.004	101.2	MP-91-1.19 Fluorite 1.6
7	0.01	0.002	52.6	BD	46.5	0.008	0.004	0	99.1	MP-91-1.19 Fluorite 1.7
8	BD	BD	52.5	0.06	46.2	0.012	BD	BD	98.7	MP-91-1.19 Fluorite 1.8
9	BD	BD	52.5	BD	45.9	BD	BD	BD	98.3	MP-91-1.19 Fluorite 1.9
10	BD	0.001	52.6	0	46.2	BD	BD	BD	98.7	MP-91-1.19 Fluorite 1.10
11	BD	0.012	48.9	1.80	43.9	0.03	0.01	0.77	95.5	MP-91-1.19 Fluorite 2.1
12	0.001	0.001	52.1	0.03	46.1	BD	0.02	0.14	98.4	MP-91-1.19 Fluorite 2.2
13	0.011	BD	51.6	0.29	47.0	0.006	BD	0.12	99.0	MP-91-1.19 Fluorite 2.3
14	BD	BD	51.4	0.07	46.4	0.008	0	0.19	98.0	MP-91-1.19 Fluorite 2.4
15	0.04	0.002	51.9	0.05	46.7	0.013	BD	0.17	98.8	MP-91-1.19 Fluorite 2.5
16	0.03	BD	53.4	BD	46.4	0.003	BD	0.09	100.0	MP-91-1.19 Fluorite 2.6
17	BD	BD	52.9	BD	47.1	BD	BD	0.03	100.0	MP-91-1.19 Fluorite 2.7
18	0.03	0.01	51.7	0.08	46.8	0.013	0.04	0.19	98.9	MP-91-1.19 Fluorite 2.8
19	0.00	BD	52.3	0.004	47.2	BD	BD	0.02	99.5	MP-91-1.19 Fluorite 2.9
20	0.01	BD	52.4	BD	45.8	BD	0.03	0.10	98.3	MP-91-1.19 Fluorite 2.10

Fluorite analyses performed via EPMA. BD represents values that were below the detection limit of the instrument. In wt% oxide. Text in red denotes anomalous analyses (low total): they were not used in subsequent calculations.

Table A.3: EPMA analyses of topaz from Mount Pleasant

No.	FeO	F	Cl	TiO_2	MnO	SiO_2	MgO	Al_2O_3	Total	Comment
1	0.05	17.8	BD	0.01	BD	32.9	BD	55.1	98.4	MP-91-1.36 Topaz 1.1
2	0.08	18.0	0.034	BD	BD	33.5	BD	55.6	99.6	MP-91-1.36 Topaz 1.2
3	0.04	17.8	0.01	0.03	0.0735	32.8	BD	55.0	98.3	MP-91-1.36 Topaz 1.3
4	0.01	17.7	0.011	BD	0.017	32.7	0.021	54.9	97.8	MP-91-1.36 Topaz 1.4
5	0.03	17.8	0.019	BD	BD	33.2	BD	54.6	98.2	MP-91-1.36 Topaz 1.5
6	0.01	18.1	BD	0.04	BD	33.0	BD	55.0	98.5	MP-91-1.36 Topaz 1.6
7	0.07	17.6	BD	BD	BD	32.8	0.012	55.4	98.5	MP-91-1.36 Topaz 1.7
8	0.03	17.6	0.013	0.02	0.0339	33.3	0.020	55.4	99.1	MP-91-1.36 Topaz 1.8
9	0.05	18.0	BD	BD	BD	33.0	BD	55.5	98.7	MP-91-1.36 Topaz 1.9
10	BD	17.8	0.008	0.00	BD	33.2	BD	54.7	98.2	MP-91-1.36 Topaz 1.10
11	0.05	18.0	BD	0.06	BD	32.9	0.014	54.8	98.2	MP-91-1.36 Topaz 2.1
12	0.05	17.7	BD	BD	BD	32.9	BD	55.1	98.2	MP-91-1.36 Topaz 2.2
13	BD	17.9	BD	0.01	0.0339	32.7	0.008	54.6	97.7	MP-91-1.36 Topaz 2.3
14	BD	17.8	0.01	BD	BD	33.0	0.018	54.8	97.9	MP-91-1.36 Topaz 2.4
15	0.02	17.8	BD	0.03	BD	33.3	BD	55.1	98.7	MP-91-1.36 Topaz 2.5
16	0.08	17.1	BD	BD	0.0283	32.5	BD	54.6	97.1	MP-91-1.36 Topaz 2.6
17	0.04	17.8	BD	BD	BD	33.6	0.004	55.8	99.7	MP-91-1.36 Topaz 2.7
18	0.13	17.2	BD	0.03	0.0679	32.8	0.004	54.6	97.6	MP-91-1.36 Topaz 2.8
19	0.01	17.1	BD	BD	BD	32.7	0.011	54.2	96.7	MP-91-1.36 Topaz 2.9
20	0.05	17.7	BD	0.01	BD	33.0	BD	54.6	97.8	MP-91-1.36 Topaz 2.10
21	0.01	18.1	BD	0.02	0.12	32.6	BD	54.7	97.8	MP-91-1.36 Topaz 2.11

Topaz analyses performed via EPMA. BD represents values that were below the detection limit of the instrument. In wt% oxide. Text in red denotes anomalous analyses (low total): they were not used in subsequent calculations.

Table A.4: EPMA analyses of micas and amphiboles from Thomas Range and Pine Grove

No.	Na_2O	K2O	CaO	FeO	F	Rb_2O	Cl	TiO_2	MnO	SiO_2	MgO	Al_2O_3	Total	Comment
1	0.04	9.2	0.15	4.6	0.3	0.26	0.01	0.3	0.0	50.4	1.6	25.8	92.6	Pine 7 Tbpa Bt#1
2	0.1	8.4	0.18	4.4	0.0	0.12	0.01	1.9	0.2	53.8	1.4	24.9	95.4	Pine 7 Tbpa Bt#1
3	0.11	9.6	0.12	4.2	0.2	0.21	BD	0.3	0.0	50.2	1.6	27.1	93.5	Pine 7 Tbpa Bt#1
4	0.11	9.4	0.13	4.5	0.1	0.16	BD	0.4	0.1	51.1	1.6	26.1	93.5	Pine 7 Tbpa Bt#1
5	0.06	8.3	0.15	19.0	0.1	0.85	0.01	0.1	0.0	45.4	3.8	13.5	91.3	Pine 7 Tbpa Bt#1 Inc
6	0.09	7.8	0.12	21.5	0.2	2.5	0.02	0.0	0.1	42.6	4.6	13.8	93.2	Pine 7 Tbpa Bt#1 Inc
7	0.07	6.3	1.2	18.2	0.3	1.1	0.01	0.1	5.5	41.4	3.9	10.3	88.2	Pine 7 Tbpa Bt#1 Inc
8	0.07	5.7	1.7	16.5	0.2	1.0	0.00	0.2	8.6	38.2	3.4	10.4	85.8	Pine 7 Tbpa Bt#1 Inc

9	1.9	1.2	9.8	28.7	0.5	BD	0.22	2.0	0.6	38.4	3.3	8.5	94.9	Pine 7 Tbpa Amp#1
10	1.9	1.2	10.1	29.2	0.2	0.03	0.22	2.0	0.5	40.4	3.5	8.7	97.8	Pine 7 Tbpa Amp#1
11	1.9	1.1	10.0	28.1	0.8	BD	0.22	2.0	0.6	40.9	3.6	8.6	97.3	Pine 7 Tbpa Amp#1
12	1.8	1.1	9.9	28.7	0.1	0.04	0.23	2.0	0.5	40.8	3.6	8.3	96.9	Pine 7 Tbpa Amp#1
13	2.0	1.1	9.6	29.2	0.3	0.07	0.23	1.9	0.5	40.8	3.4	8.7	97.6	Pine 7 Tbpa Amp#2
14	2.1	1.2	9.9	29.4	0.4	0.16	0.25	2.1	0.6	40.2	3.2	9.2	98.4	Pine 7 Tbpa Amp#2
15	1.9	1.1	9.8	26.6	0.5	0.06	0.21	1.9	0.6	32.0	4.4	7.7	86.6	Pine 7 Tbpa Amp#3
16	1.8	1.1	9.8	25.9	0.8	0.10	0.16	1.9	0.5	32.5	4.7	7.6	86.5	Pine 7 Tbpa Amp#3
17	0.01	4.2	1.8	28.2	0.1	0.36	0.04	0.3	BD	44.7	1.1	6.4	87.1	Pine 7 Tbpa Bt#2
18	0.08	4.1	1.9	28.1	BD	0.42	0.03	0.3	0.0	44.3	1.0	6.8	86.9	Pine 7 Tbpa Bt#2
19	0.08	9.3	0.16	1.5	0.2	0.13	0.00	0.2	0.1	49.3	0.5	33.6	94.9	Pine 2 Tpg Mica#1
20	0.04	9.3	0.25	1.1	0.3	0.26	BD	0.1	0.1	49.4	0.6	34.3	95.6	Pine 2 Tpg Mica#1
21	0.10	9.5	0.14	1.3	0.4	0.34	0.00	0.1	0.0	49.2	0.6	33.9	95.4	Pine 2 Tpg Mica#1
22	0.08	9.4	0.12	1.3	0.3	0.04	BD	0.0	0.0	48.0	0.5	34.6	94.3	Pine 2 Tpg Mica#1
23	0.10	9.5	0.15	1.3	0.4	0.11	0.01	0.2	0.1	48.6	0.5	33.5	94.3	Pine 2 Tpg Mica#2
24	0.10	9.4	0.19	1.4	0.1	0.09	BD	0.1	0.1	49.1	0.5	33.9	95.1	Pine 2 Tpg Mica#2
25	0.11	9.6	0.18	1.6	0.5	0.24	0.02	0.1	0.1	48.5	0.6	33.9	95.2	Pine 2 Tpg Mica#2
26	0.09	9.5	0.15	1.5	0.0	0.24	0.01	0.2	0.1	48.5	0.4	33.7	94.5	Pine 2 Tpg Mica#2
27	0.08	9.5	0.17	1.3	0.0	0.15	0.00	0.1	0.1	48.4	0.5	34.0	94.2	Pine 2 Tpg Mica#3
28	0.09	9.2	0.13	1.3	0.4	0.16	0.00	0.2	0.1	50.7	0.5	32.0	94.7	Pine 2 Tpg Mica#3
29	0.08	9.4	0.08	1.7	BD	0.25	0.01	0.2	0.1	49.1	0.6	32.8	94.3	Pine 2 Tpg Mica#3
30	0.10	9.5	0.17	1.6	0.0	0.35	0.00	0.1	0.2	49.0	0.5	34.0	95.5	Pine 2 Tpg Mica#3
31	0.40	8.8	0.02	16.7	2.6	0.07	0.08	3.6	0.6	37.1	13.0	13.4	95.2	NMNH 109593-13 Bt#1
32	0.42	9.3	0.16	16.0	3.1	0.12	0.09	3.7	0.6	36.9	13.9	14.0	97.0	NMNH 109593-13 Bt#1
33	0.35	9.3	BD	17.4	1.1	0.13	0.07	3.6	0.5	35.3	12.9	14.2	94.4	NMNH 109593-13 Bt#2
34	0.41	9.2	BD	18.0	2.4	0.02	0.07	3.5	0.7	35.8	12.8	14.0	95.8	NMNH 109593-13 Bt#2
35	0.45	9.2	0.01	17.4	2.2	0.06	0.07	3.4	0.7	36.8	13.3	13.7	96.4	NMNH 109593-13 Bt#2
36	0.37	8.9	0.01	17.0	1.3	0.06	0.06	3.6	0.6	36.4	12.8	14.1	94.6	NMNH 109593-13 Bt#2
37	0.44	9.0	0.03	17.5	2.9	0.12	0.08	3.9	0.5	36.1	13.4	13.8	96.5	NMNH 109593-13 Bt#3
38	0.40	8.7	BD	18.3	1.6	0.02	0.08	3.9	0.6	35.3	12.2	14.1	94.6	NMNH 109593-13 Bt#3
39	0.41	9.0	BD	17.9	1.3	0.06	0.07	3.8	0.6	35.7	12.7	14.1	95.0	NMNH 109593-13 Bt#3
40	0.41	9.4	0.04	17.2	1.8	BD	0.08	3.4	0.5	35.2	13.4	13.4	93.9	NMNH 109593-13 Bt#4
41	0.41	9.5	0.01	17.4	1.4	0.09	0.07	3.5	0.7	35.3	13.7	13.2	94.7	NMNH 109593-13 Bt#4
42	0.39	9.5	BD	17.5	2.0	0.10	0.07	3.4	0.6	37.5	13.8	14.4	98.4	NMNH 109593-13 Bt#4

Mica and amphibole analyses performed via EPMA. BD represents values that were below the detection limit of the instrument. In wt% oxide. Text in red denotes anomalous analyses (low total): they were not used in subsequent calculations.

Table A.5: EPMA analyses of micas from Climax

No.	SiO_2	TiO_2	Al_2O_3	FeO	MnO	MgO	CaO	Na_2O	K2O	Rb_2O	F	Cl	Total	Comment
1	38.6	1.23	17.91	14.12	2.66	8.49	BD	0.19	9.77	0.87	0.96	0.03	94.37	719r Dark Mica #1
2	38.6	1.20	17.13	14.28	2.27	9.46	BD	0.14	9.98	0.85	2.35	0.02	95.26	719r Dark Mica #1
3	47.8	0.30	26.44	2.92	1.35	3.03	BD	0.14	10.96	1.09	4.14	0.00	96.41	719r Light Mica #1
4	47.6	0.25	25.99	3.19	1.23	3.26	0.02	0.11	10.91	0.99	3.95	0.00	95.81	719r Light Mica #1
5	47.6	0.34	26.17	3.10	1.00	3.60	BD	0.13	10.79	0.74	4.03	0.02	95.84	719r Light Mica #1
6	46.0	0.52	28.24	3.93	0.57	2.55	0.04	0.22	10.38	0.68	3.35	0.01	95.11	719r Light Mica #2
7	45.2	0.65	27.49	5.32	0.77	2.70	BD	0.24	10.58	0.61	2.52	0.01	95.03	719r Light Mica #2
8	48.4	0.37	28.70	1.65	0.49	3.22	0.01	0.21	10.81	0.56	3.84	0.00	96.60	719r Light Mica #3
9	48.4	0.48	26.81	1.91	0.36	3.60	0.01	0.21	10.54	0.50	4.42	0.01	95.40	719r Light Mica #3
10	48.4	0.35	28.46	0.79	0.37	3.46	0.04	0.17	10.83	0.59	3.71	0.00	95.58	719r Light Mica #4
11	45.2	0.53	26.66	5.42	0.75	2.78	BD	0.35	10.37	0.62	2.62	0.01	94.16	719r Light Mica #4
12	44.5	0.64	26.42	6.06	1.11	2.80	BD	0.23	10.38	0.60	1.57	0.01	93.63	719r Light Mica #5
13	44.5	0.57	26.29	6.74	1.23	3.24	BD	0.39	10.31	0.78	1.83	0.00	95.04	719r Light Mica #5
14	95.4	BD	0.004	BD	BD	BD	0.012	0.02	0.00	0.15	0.00	0.04	95.59	720r Light Mica #1
15	45.5	0.30	32.72	3.00	0.26	0.60	0.04	0.45	10.45	0.42	2.11	0.00	94.96	720r Light Mica #1
16	47.5	0.27	28.60	1.75	0.11	3.24	0.01	0.36	10.93	0.61	4.60	0.00	96.00	720r Light Mica #2
17	47.6	0.39	28.46	1.83	0.11	3.21	0.01	0.34	10.88	0.50	4.40	0.00	95.90	720r Light Mica #2
18	39.9	1.54	16.79	12.46	1.30	10.76	BD	0.18	10.06	0.46	2.18	0.03	94.71	721r Dark Mica #1
19	39.7	1.56	16.88	12.33	1.38	10.66	BD	0.20	9.95	0.52	3.00	0.03	94.95	721r Dark Mica #1
20	30.0	1.50	14.66	12.77	1.22	11.01	BD	0.15	9.67	0.48	2.66	0.03	83.02	721r Dark Mica #2
21	39.4	1.55	16.69	12.37	1.39	10.82	BD	0.19	10.12	0.75	2.77	0.03	94.81	721r Dark Mica #2
22	41.0	1.12	17.68	10.86	1.51	8.82	BD	0.16	10.16	0.70	2.74	0.02	93.66	721r Dark Mica #3
23	41.2	1.35	17.93	11.73	1.64	8.92	0.01	0.22	10.07	0.73	2.88	0.02	95.44	721r Dark Mica #3
24	39.9	1.34	16.78	11.89	1.38	10.82	0.02	0.24	9.97	0.54	2.63	0.02	94.40	721r Dark Mica #4
25	39.4	1.19	16.37	11.94	1.47	10.60	0.01	0.21	10.14	0.69	2.62	0.03	93.54	721r Dark Mica #4
26	37.7	2.21	17.09	16.00	3.15	7.21	BD	0.24	9.87	0.10	0.21	0.03	93.72	722r Dark Mica #1
27	38.8	1.53	17.06	14.79	2.91	7.92	BD	0.27	10.05	0.47	1.25	0.05	94.55	722r Dark Mica #1
28	37.5	1.16	18.79	15.38	2.87	4.71	0.03	0.15	9.58	1.38	0.00	0.07	91.50	722r Dark Mica #2
29	38.6	1.26	19.30	15.27	3.02	4.67	0.07	0.13	9.79	1.04	0.00	0.04	93.01	722r Dark Mica #2
30	38.2	1.42	18.40	15.08	2.80	6.71	BD	0.19	9.67	1.21	0.44	0.05	94.00	722r Dark Mica #3
31	37.0	1.25	18.10	15.67	2.76	6.73	BD	0.15	9.74	0.93	0.17	0.03	92.41	722r Dark Mica #3
32	37.7	1.22	18.86	15.99	2.89	5.14	0.01	0.19	9.78	1.40	0.21	0.05	93.35	722r Dark Mica #4
33	38.8	1.10	19.43	14.56	3.02	4.82	BD	0.18	9.88	1.34	0.84	0.03	93.63	722r Dark Mica #4
34	45.6	0.37	25.67	6.72	1.05	3.30	BD	0.19	10.75	1.08	3.35	0.01	96.72	722r Light Mica #1
35	45.2	0.40	25.70	6.65	1.05	3.26	0.08	0.19	10.59	1.06	3.03	0.00	95.91	722r Light Mica #1
36	36.7	1.74	15.70	15.74	0.71	12.00	BD	0.01	9.83	0.42	0.00	0.07	92.73	723r Dark Mica #1

37	37.2	1.82	15.64	16.47	0.75	12.05	BD	0.06	9.82	0.37	0.00	0.06	93.97	723r Dark Mica #1
38	36.1	1.81	17.45	18.48	0.49	10.58	BD	0.12	9.91	0.37	0.00	0.13	95.11	723r Dark Mica #2
39	36.7	1.79	17.31	17.54	0.46	10.97	0.01	0.11	9.95	0.50	0.00	0.09	95.13	723r Dark Mica #2
40	37.8	1.46	15.52	16.41	0.49	12.87	BD	0.18	9.86	0.56	0.00	0.10	95.02	723r Dark Mica #3
41	37.5	1.61	15.89	16.23	0.38	12.26	BD	0.14	9.79	0.47	0.00	0.09	94.19	723r Dark Mica #3
42	37.6	1.54	15.57	16.27	0.49	12.40	BD	0.09	9.82	0.35	0.00	0.09	94.08	723r Dark Mica #4
43	37.4	2.81	15.87	15.97	0.44	12.53	BD	0.08	9.78	0.44	0.00	0.07	95.19	723r Dark Mica #4
44	38.3	1.01	14.57	13.55	0.47	14.53	BD	0.10	10.12	0.42	0.85	0.06	93.62	723r Dark Mica #5
45	38.5	1.01	14.67	13.95	0.46	14.40	0.02	0.11	10.05	0.51	0.67	0.04	94.05	723r Dark Mica #5
46	37.5	1.80	15.77	16.47	0.41	11.75	BD	0.15	10.03	0.40	0.00	0.11	94.18	723r Dark Mica #6
47	44.2	0.12	33.43	0.77	0.57	0.17	BD	0.08	10.82	0.27	0.54	0.01	90.69	725r Light Mica #1
48	47.4	0.12	32.40	0.69	0.44	1.32	BD	0.04	10.53	0.25	1.12	0.01	93.87	725r Light Mica #1
49	46.6	0.11	33.18	0.85	0.43	1.02	BD	0.03	10.96	0.48	1.40	0.00	94.50	725r Light Mica #2
50	45.4	0.13	36.09	0.50	0.32	0.16	BD	0.05	11.16	0.45	0.38	0.00	94.52	725r Light Mica #2
51	45.9	0.51	30.70	4.02	0.30	1.50	BD	0.35	10.69	1.12	1.99	0.03	96.22	725r Light Mica #3
52	46.09	0.46	29.53	3.35	0.51	1.98	BD	0.30	10.75	1.03	2.31	0.01	95.34	725r Light Mica #3

Mica analyses performed via EPMA. BD represents values that were below the detection limit of the instrument. In wt% oxide. Text in red denotes anomalous analyses (hit quartz): they were not used in subsequent calculations.

Appendix B: LA-ICP-MS Analyses

Table B.1: LA-ICP-MS analyses of micas and topaz from Mount Pleasant

		MP-91-1.36										
		biotite 4	**biotite 4**	**biotite 4**	**biotite 2**	**biotite 2**	**biotite 2**	**biotite 5**	**biotite 5**	**biotite 5**	**topaz 1**	**topaz 1**
Li	**6**	10476	10412	10570	12934	13471	11949	11423	11835	12618	BD	BD
Li	**7**	11117	11794	12207	14459	14692	13265	12381	13457	13763	BD	BD
Be	**9**	31	32	31	43	37	33	35	31	41	BD	BD
Sc	**45**	27	24	33	20	21	23	27	26	23	BD	BD
Cr	**53**	BD	BD	BD	BD	BD	BD	BD	BD	BD	BD	BD
Zn	**67**	452	482	545	417	479	467	448	430	394	BD	BD
Ga	**69**	54	65	85	44	54	57	54	50	41	BD	BD
Rb	**85**	7496	9220	9443	8524	9328	8883	8141	9062	8908	BD	BD
Sr	**88**	0.51	3.9	0.26	0.28	0.26	0.51	0.31	BD	0.23	BD	BD
Y	**89**	0.57	0.06	24	0.20	0.51	1.1	0.20	BD	0.01	BD	BD
Zr	**90**	0.62	0.29	0.26	0.31	0.34	0.36	0.63	0.11	0.07	BD	BD
Nb	**93**	251	271	343	93	214	265	280	263	86	BD	0.21
Mo	**97**	0.52	0.73	0.54	0.45	0.49	0.25	0.37	0.52	0.37	BD	BD
Cd	**111**	BD	BD	BD	0.25	BD	0.20	0.11	0.10	BD	BD	BD
In	**115**	0.94	1.1	1.2	0.69	0.86	1.2	0.97	1.2	0.70	BD	BD
Sn	**118**	198	207	246	103	166	231	222	213	84	BD	BD

Cs	**133**	297	321	391	486	296	274	650	415	837	BD	BD
La	**139**	0.07	0.01	0.02	0.03	0.05	0.01	0.03	BD	0.004	0.26	BD
Ce	**140**	0.14	0.04	0.04	0.04	0.08	BD	0.04	0.00	BD	BD	BD
Pr	**141**	0.01	0.02	0.01	0.00	0.01	0.02	0.01	0.00	BD	BD	BD
Nd	**146**	0.10	0	0.03	0.02	0	0.02	0	0.04	BD	BD	BD
Sm	**147**	0.03	0.04	0.06	0.02	0.04	BD	BD	BD	BD	BD	BD
Eu	**151**	BD	BD	BD	BD	BD	BD	BD	0.01	BD	BD	BD
Gd	**157**	BD	BD	0.22	0.04	BD	0.08	BD	0.04	0.13	BD	BD
Tb	**159**	BD	0.002	0.23	0	0.02	0.01	BD	BD	BD	BD	BD
Dy	**163**	0.06	0.01	3.2	0.04	0.07	0.09	0.04	BD	BD	BD	BD
Ho	**165**	0.004	BD	1.0	BD	0.02	BD	0.01	BD	BD	BD	BD
Er	**166**	0.06	BD	5.1	BD	0.04	0.13	0.03	0.01	BD	BD	BD
Tm	**169**	0.02	0.00	0.92	0.01	0.02	0.03	0	BD	BD	BD	BD
Yb	**172**	0.11	0.01	6.13	0.01	0.19	0.33	0.04	BD	0.01	BD	BD
Lu	**175**	0.03	0.01	1.13	0.00	0.04	0.11	0.004	BD	0.004	BD	BD
Hf	**178**	0.08	0.05	0.04	0.05	0.05	0.05	0.01	0.08	0.01	BD	BD
Ta	**181**	44	43	17	14	57	56	66	68	9.5	BD	BD
W	**183**	20	18	19	18	23	28	19	27	20	BD	BD
Th	**232**	0.17	0.05	0.13	0.06	0.16	0.07	0.003	0.03	0.009	BD	BD
U	**238**	0.07	0.08	0.61	0.05	0.06	0.13	0.10	0.07	0.01	BD	BD

MP-91-1.36

		topaz 1	**biotite 1**	**biotite 1**	**biotite 1**	**biotite 3**	**biotite 3**	**biotite 3**
Li	**6**	BD	12303	12947	12018	12234	14042	12031
Li	**7**	BD	14448	14992	13919	14587	15225	13595
Be	**9**	6	35	37	41	37	40	36
Sc	**45**	BD	23	22	24	27	31	29
Cr	**53**	BD	BD	BD	BD	BD	BD	BD
Zn	**67**	BD	456	415	445	406	412	458
Ga	**69**	19	56	51	58	54	58	51
Rb	**85**	977	10211	9844	8682	9287	9309	8073
Sr	**88**	6.0	0.49	BD	0.58	0.11	BD	BD
Y	**89**	21	1.1	0.01	0.67	BD	0.06	BD
Zr	**90**	1.2	1.0	0.10	0.64	0.10	0.14	0.19
Nb	**93**	16	236	199	327	80	164	222
Mo	**97**	BD	BD	0.42	0.49	0.34	0.32	0.37
Cd	**111**	0.85	0.10	0.06	0.11	BD	0.26	BD
In	**115**	0.18	1.1	1.1	0.98	0.81	0.91	0.82
Sn	**118**	33	168	149	170	122	162	183
Cs	**133**	40	530	526	581	817	887	369
La	**139**	0.93	0.19	0.01	0.18	0.00	0.01	BD
Ce	**140**	5.0	0.44	0.02	BD	0.00	0.03	0.00
Pr	**141**	0.48	0.09	0.01	0.03	BD	0.01	0.01

Nd	**146**	1.8	0.17	0.02	0.04	BD	BD	0.02
Sm	**147**	0.42	0.05	BD	0.08	BD	BD	BD
Eu	**151**	BD	BD	BD	0.01	0.01	0.01	BD
Gd	**157**	0.36	BD	BD	BD	BD	BD	BD
Tb	**159**	0.32	0.02	0.01	0.02	BD	0.003	BD
Dy	**163**	2.58	0.21	BD	0.07	0.01	BD	BD
Ho	**165**	0.43	0.05	BD	0.04	BD	BD	BD
Er	**166**	2.37	0.19	BD	0.12	BD	0.02	BD
Tm	**169**	0.69	0.02	BD	0.04	BD	0.003	BD
Yb	**172**	9.17	0.18	BD	0.15	BD	0.01	BD
Lu	**175**	1.76	0.06	BD	0.04	0.003	0.003	BD
Hf	**178**	0.0	0.15	BD	0.07	0.03	0.01	0.08
Ta	**181**	2.4	43	45	35	3.4	12	49
W	**183**	1.2	20	17	17	18	20	27
Th	**232**	0.60	0.15	0.00	0.21	0.004	0.02	0.02
U	**238**	0.04	0.33	0.04	0.21	0.05	0.08	0.07

Mica and topaz analyses performed via LA-ICP-MS. BD represents values that were below the detection limit of the instrument. In parts per million (ppm).

Table B.2: LA-ICP-MS analyses of biotite from Thomas Range

							NMNH 109593-10					
		biotite 5	**biotite 5**	**biotite 1**	**biotite 1**	**biotite 1**	**biotite 2**	**biotite 3**	**biotite 3**	**biotite 3**	**biotite 4**	**biotite 4**
Li	**6**	380	521	422	395	460	2579	416	304	384	1537	1645
Li	**7**	362	516	397	379	403	2736	377	BD	BD	1628	1763
Be	**9**	5.5	5.1	6.0	7.1	5.0	2.6	4.3	5.2	4.3	4.2	3.6
Sc	**45**	29	39	25	20	19	73	23	16	18	64	60
Cr	**53**	BD	BD	BD	BD	BD	BD	BD	BD	BD	BD	BD
Zn	**67**	648	659	584	633	574	835	614	514	563	786	736
Ga	**69**	39	32	31	66	54	41	30	29	29	40	55
Rb	**85**	723	754	712	739	748	2391	697	691	729	872	877
Sr	**88**	9.5	2.8	2.0	12.6	13.6	1.4	2.3	1.6	1.6	3.1	12.8
Y	**89**	1.9	1.7	1.7	1.1	1.1	0.9	1.7	1.3	1.6	3.7	2.8
Zr	**90**	4.7	5.7	5.0	4.1	3.9	11.6	5.2	4.0	4.3	7.0	7.8
Nb	**93**	194	199	198	194	195	1223	189	176	188	274	299
Mo	**97**	1.6	1.9	2.3	1.6	1.5	25	BD	2.4	BD	4.3	6.4
Cd	**111**	BD	0.34	BD	0.14	BD	BD	BD	0.31	0	0.10	BD
In	**115**	0.19	0.22	0.30	0.38	0.47	0.27	0.30	0.20	0.15	0.29	0.25
Sn	**118**	2.4	2.5	5.0	5.0	6.5	7.2	3.4	3.2	3.7	4.3	5.2
Cs	**133**	10	9.9	11	10	10	52	12	12	11	9.1	12
La	**139**	2.2	1.5	0.74	0.89	1.2	1.4	1.1	0.81	0.84	2.7	4.0
Ce	**140**	7.5	6.1	5.7	3.9	4.5	19	7.4	6.4	6.9	13	20

Pr	**141**	0.59	0.44	0.25	0.26	0.45	0.37	0.42	0.30	0.36	0.90	1.7
Nd	**146**	1.79	1.39	0.80	0.92	1.30	0.99	0.69	0.63	1.0	2.5	4.3
Sm	**147**	0.38	0.32	0.27	0.21	0.27	0.06	0.36	0.29	0.34	0.61	0.71
Eu	**151**	0.02	BD	0.005	0.01	0.01	0.02	0.02	0.01	0.01	0	0
Gd	**157**	0.31	0.24	0.12	0.23	0.23	0.10	0.36	0.12	0.34	0.51	BD
Tb	**159**	0.08	0.10	0.04	0.03	0.02	0.06	0.04	0.04	0.06	0.07	0.11
Dy	**163**	0.35	0.26	0.34	0.20	0.29	0.12	0.43	0.23	0.41	0.53	0.56
Ho	**165**	0.12	0.08	0.10	0.06	0.06	0.02	0.12	0.06	0.07	0.11	0.12
Er	**166**	0.32	0.34	0.33	0.21	0.17	0.18	0.24	0.19	0.33	0.54	0.41
Tm	**169**	0.05	0.06	0.07	0.03	0.04	0.06	0.05	0.02	0.07	0.10	0.07
Yb	**172**	0.64	0.44	0.52	0.26	0.38	0.25	0.49	0.40	0.47	0.49	0.52
Lu	**175**	0.10	0.08	0.07	0.05	0.02	0.02	0.09	0.08	0.09	0.10	0.08
Hf	**178**	0.2	0.2	0.2	0.1	0.1	1.0	0.1	0.2	0.1	0.4	0.5
Ta	**181**	3.5	3.8	3.2	3.3	3.2	76.5	3.4	3.4	3.3	5.9	8.1
W	**183**	2.6	3.2	3.2	1.6	1.4	12.0	3.6	3.6	3.3	2.9	1.8
Th	**232**	19.9	19.0	9.6	8.2	5.4	13.9	15.1	8.5	11.3	6.2	6.8
U	**238**	0.7	0.9	1.4	0.7	0.4	1.7	1.5	1.0	1.2	1.4	2.1

Mica and topaz analyses performed via LA-ICP-MS. BD represents values that were below the detection limit of the instrument. In parts per million (ppm).

Table B.3: LA-ICP-MS analyses of micas and amphiboles from Thomas Range and Pine Grove

		NMNH 109593-13						Pine 7 Tbpa		
		Biotite 2	**Biotite 2**	**Biotite 2**	**Biotite 1**	**Biotite 1 Incl**	**Biotite 1 Incl**	**Amphibole 1**	**Amphibole 1**	**Amphibole 2**
Li	**6**	BD	15.50	55.35	106.03	86.71	33.54	7.48	6.98	5.89
Li	**7**	BD	BD	BD	BD	BD	BD	BD	BD	BD
Be	**9**	0.59	0.63	BD	0.69	11.07	32.16	3.64	5.65	8.13
Sc	**45**	27.28	31.28	27.24	37.38	7.35	5.76	340.79	329.39	338.52
Cr	**53**	BD	BD	BD	BD	BD	42.35	BD	BD	BD
Zn	**67**	674.88	1803.78	858.74	605.79	574.15	592.65	643.28	664.20	675.30
Ga	**69**	190.01	1225.08	428.92	197.06	74.72	190.46	27.61	28.81	38.71
Rb	**85**	830.71	473.50	569.77	584.28	8449.52	5065.30	BD	BD	BD
Sr	**88**	5.83	9.35	4.05	23.48	18.69	12.28	6.06	5.77	9.16
Y	**89**	0.12	0.29	0.18	BD	226.57	9.50	437.89	447.34	1044.93
Zr	**90**	3.14	2.44	2.07	7.81	21.55	4.91	91.33	90.42	136.00
Nb	**93**	62.86	57.35	54.13	72.74	591.11	30.50	344.39	339.17	1154.02
Mo	**97**	0.55	0.36	0.15	0.72	0.35	BD	2.03	2.20	1.11
Cd	**111**	0.06	BD	0.05	BD	12.94	BD	BD	BD	1.31
In	**115**	0.15	0.21	0.17	0.24	0.31	0.07	2.48	2.72	6.19
Sn	**118**	5.63	7.19	5.87	6.22	62.92	14.28	3.47	3.69	8.14
Cs	**133**	29.66	11.77	16.43	15.56	979.01	543.57	BD	BD	0.98
La	**139**	0.03	0.06	0.02	0.32	22.38	0.23	67.62	68.37	58.41

Ce	**140**	0.03	0.01	0.00	0.53	556.35	0.10	330.04	315.61	315.37
Pr	**141**	0.02	0.00	BD	0.04	7.22	0.06	68.05	66.40	77.21
Nd	**146**	BD	0.04	0.04	0.03	28.82	0.03	378.98	384.65	495.54
Sm	**147**	0.03	BD	0.02	BD	18.32	0.22	149.63	149.32	303.83
Eu	**151**	0.07	0.30	BD	0.02	0.03	0.01	0.51	0.71	0.32
Gd	**157**	0.02	0.02	0.08	BD	28.43	0.76	143.50	141.69	378.40
Tb	**159**	BD	0.00	0.01	0.00	7.20	0.10	21.66	21.70	59.74
Dy	**163**	BD	BD	BD	0.06	56.76	1.04	117.17	121.70	338.13
Ho	**165**	0.00	BD	BD	BD	11.51	0.27	20.49	19.14	53.75
Er	**166**	BD	BD	BD	0.03	35.90	1.17	47.18	48.23	113.94
Tm	**169**	0.00	BD	BD	BD	4.44	0.18	5.34	5.43	11.08
Yb	**172**	BD	BD	0.01	BD	24.11	2.23	28.63	30.00	58.65
Lu	**175**	0.01	0.01	0.00	BD	3.17	0.39	3.89	4.11	7.64
Hf	**178**	0.11	0.12	0.15	0.30	0.72	0.02	5.62	5.54	9.98
Ta	**181**	1.09	0.96	0.95	1.35	0.88	BD	5.12	4.72	9.79
W	**183**	0.30	0.07	0.24	0.39	6.97	0.22	0.07	0.02	0.06
Th	**232**	0.46	0.03	0.15	0.76	95.12	0.87	1.09	0.85	1.57
U	**238**	0.08	0.03	0.06	0.08	80.23	21.78	0.22	0.18	0.55

		Pine 7 Tbpa					NMNH109593-13				
		Amphibole 2	**Amphibole 2**	**Amphibole 3**	**Amphibole 3**	**Amphibole 3**	**Biotite3**	**Biotite3**	**Biotite3**	**Biotite3**	**Biotite 4**
Li	**6**	20.46	13.22	BD	BD	BD	25.65	BD	BD	79.34	35.52
Li	**7**	BD	BD	BD	BD	BD	BD	BD	BD	BD	BD
Be	**9**	9.01	7.41	3.95	3.27	3.69	0.90	1.11	BD	BD	0.12
Sc	**45**	353.43	327.18	204.96	201.14	192.15	34.95	35.45	37.63	34.84	29.34
Cr	**53**	BD	BD	BD	BD	BD	14.24	9.69	BD	16.83	12.53
Zn	**67**	709.95	651.41	537.70	479.44	514.77	3856.02	3795.42	5192.57	3209.41	663.21
Ga	**69**	36.22	34.34	25.16	24.29	24.56	123.15	2641.57	2027.10	2308.87	197.04
Rb	**85**	BD	BD	BD	BD	BD	303.58	428.94	328.99	326.45	539.93
Sr	**88**	10.30	14.62	13.52	13.41	16.64	6.49	6.25	5.66	7.54	3.82
Y	**89**	831.45	818.68	330.99	316.48	351.12	0.54	3.44	0.78	0.51	0.04
Zr	**90**	110.81	102.58	72.17	71.33	76.68	3.33	4.47	3.67	7.50	2.32
Nb	**93**	714.47	695.10	215.23	205.93	233.08	88.50	73.96	85.51	75.52	70.03
Mo	**97**	1.11	1.57	2.41	BD	1.65	0.27	0.53	0.40	0.41	0.35
Cd	**111**	1.51	1.39	0.80	0.72	0.86	0.03	BD	BD	0.17	BD
In	**115**	4.89	3.69	2.03	1.75	1.96	0.18	0.21	0.29	0.27	0.19
Sn	**118**	8.86	6.60	2.75	2.84	3.56	6.95	7.11	8.16	7.82	6.14
Cs	**133**	1.73	2.08	BD	BD	BD	2.81	4.53	2.70	6.01	4.96
La	**139**	54.31	51.72	70.52	71.51	87.26	0.13	3.59	0.15	0.16	0.01
Ce	**140**	280.24	263.34	332.79	331.85	381.59	0.02	11.82	0.01	0.10	0.01
Pr	**141**	65.03	60.18	68.14	63.94	71.17	0.00	1.47	0.01	BD	BD
Nd	**146**	400.06	371.98	350.01	352.51	384.44	0.09	5.44	0.05	0.08	BD
Sm	**147**	220.85	203.85	121.91	115.16	127.27	0.01	0.96	0.00	0.01	BD

Eu	**151**	0.38	0.48	1.02	1.21	1.00	0.93	1.33	1.67	0.73	0.04
Gd	**157**	282.58	267.57	107.31	107.28	116.85	0.14	0.98	0.24	0.14	0.04
Tb	**159**	44.85	41.61	15.07	15.49	16.68	0.00	0.07	BD	0.00	BD
Dy	**163**	254.04	243.50	86.76	85.72	91.93	BD	0.79	BD	0.02	BD
Ho	**165**	42.16	39.64	14.86	14.20	15.81	0.00	0.05	0.00	0.00	0.01
Er	**166**	96.37	86.03	34.18	34.11	37.60	0.00	0.18	0.02	BD	BD
Tm	**169**	9.86	8.94	3.96	3.95	4.41	BD	0.01	BD	0.00	BD
Yb	**172**	51.74	49.18	23.26	22.37	25.29	0.02	0.29	0.04	BD	0.03
Lu	**175**	7.21	6.58	2.79	3.01	2.91	0.01	0.05	0.00	0.01	0.00
Hf	**178**	8.28	7.69	3.85	4.60	4.46	0.22	0.29	0.26	0.33	0.07
Ta	**181**	8.00	6.71	3.45	3.21	3.72	1.54	1.52	1.47	1.42	1.55
W	**183**	BD	0.12	0.06	0.02	0.06	0.06	0.23	0.20	0.24	0.15
Th	**232**	1.73	1.99	0.92	0.78	1.71	0.06	0.62	0.07	0.15	0.06
U	**238**	0.76	0.94	0.18	0.15	0.31	0.05	0.15	0.07	0.09	0.05

		NMNH109593-13		**Pine 2 Tpg**					
		Biotite 4	**Biotite 4**	**Muscovite 2**	**Muscovite 2**	**Muscovite 2**	**Muscovite 3**	**Muscovite 3**	**Muscovite 1**
Li	**6**	36.49	BD	BD	13.98	4.65	8.09	3.95	11.75
Li	**7**	BD	BD	BD	BD	BD	BD	BD	BD
Be	**9**	BD	BD	10.60	6.28	10.62	10.27	9.22	7.57
Sc	**45**	28.22	29.35	137.81	87.26	135.55	86.90	74.54	97.35
Cr	**53**	10.85	9.83	BD	BD	BD	BD	BD	BD
Zn	**67**	553.60	458.54	145.78	118.02	134.84	159.41	147.79	134.82
Ga	**69**	109.79	114.04	88.77	67.84	86.69	100.39	100.41	73.19
Rb	**85**	709.76	544.76	1056.54	815.46	1046.18	1224.10	1156.25	931.69
Sr	**88**	12.77	5.00	6.11	8.16	5.85	5.98	5.47	7.44
Y	**89**	0.05	BD	322.95	201.66	114.72	159.89	191.30	556.14
Zr	**90**	3.33	4.44	27.62	39.15	20.31	17.16	16.45	32.56
Nb	**93**	67.93	78.03	1085.78	672.42	1020.63	1006.14	510.82	964.59
Mo	**97**	0.54	0.16	0.18	0.42	0.64	0.22	0.17	BD
Cd	**111**	0.16	0.08	BD	0.41	0.04	BD	BD	0.30
In	**115**	0.24	0.26	0.59	0.35	0.49	0.48	0.35	0.57
Sn	**118**	7.18	7.24	62.41	55.58	51.87	46.62	36.61	99.04
Cs	**133**	10.60	8.28	13.38	15.16	16.42	19.77	16.91	13.53
La	**139**	0.03	0.07	0.89	0.78	0.54	0.75	0.33	1.41
Ce	**140**	0.03	0.07	10.30	6.79	3.79	6.31	5.40	20.39
Pr	**141**	0.01	0.00	1.55	1.09	0.75	0.87	0.74	3.77
Nd	**146**	0.01	0.03	12.89	8.31	5.61	6.63	6.47	31.11
Sm	**147**	0.03	0.02	25.84	16.61	9.52	10.90	14.94	51.82
Eu	**151**	0.04	0.04	0.13	0.14	BD	0.07	0.10	0.29
Gd	**157**	0.02	0.01	48.90	31.34	17.18	21.99	28.15	93.96
Tb	**159**	BD	BD	12.27	7.22	3.95	5.45	7.22	21.72
Dy	**163**	BD	BD	86.19	52.84	28.85	42.22	47.17	148.90
Ho	**165**	0.00	BD	15.27	10.18	5.36	7.63	8.87	28.22

Er	**166**	BD	0.02	43.73	27.01	14.49	19.90	25.58	75.40
Tm	**169**	0.01	BD	5.60	3.50	2.14	2.65	3.16	10.04
Yb	**172**	0.02	BD	33.48	21.06	11.51	16.84	16.77	52.71
Lu	**175**	0.01	0.01	3.66	2.30	1.50	1.98	1.90	6.14
Hf	**178**	0.10	0.23	1.72	2.33	1.94	1.41	1.20	1.87
Ta	**181**	1.46	1.61	48.01	40.26	32.85	33.24	19.20	48.26
W	**183**	0.18	0.20	37.93	38.03	24.83	33.77	18.66	43.78
Th	**232**	0.29	0.29	61.62	38.54	19.95	27.80	43.43	104.73
U	**238**	0.06	0.07	44.98	27.82	16.56	26.65	26.87	78.32

Pine 2 Tpg

		Muscovite 1	**Muscovite 1**
Li	**6**	17.19	BD
Li	**7**	BD	BD
Be	**9**	9.18	8.61
Sc	**45**	101.57	88.09
Cr	**53**	BD	BD
Zn	**67**	132.12	134.90
Ga	**69**	79.97	79.14
Rb	**85**	915.95	927.09
Sr	**88**	7.66	6.23
Y	**89**	125.63	203.41
Zr	**90**	37.28	22.90
Nb	**93**	979.54	551.15
Mo	**97**	0.04	BD
Cd	**111**	0.11	0.21
In	**115**	0.50	0.53
Sn	**118**	76.61	82.49
Cs	**133**	17.51	11.65
La	**139**	0.69	0.68
Ce	**140**	5.86	7.91
Pr	**141**	0.71	1.41
Nd	**146**	6.68	11.97
Sm	**147**	9.99	20.27
Eu	**151**	0.06	0.14
Gd	**157**	20.23	33.93
Tb	**159**	4.57	8.18
Dy	**163**	32.37	53.82
Ho	**165**	6.47	11.00
Er	**166**	16.88	27.48
Tm	**169**	2.52	3.91
Yb	**172**	13.24	21.35
Lu	**175**	1.48	2.32
Hf	**178**	2.42	1.49

Ta	**181**	40.71	29.18
W	**183**	40.08	25.36
Th	**232**	33.79	47.60
U	**238**	18.36	31.93

Mica and amphibole analyses performed via LA-ICP-MS. BD represents values that were below the detection limit of the instrument. In parts per million (ppm).

Table B.4: LA-ICP-MS analyses of micas from Climax

		dark mica 1	**dark mica 1**	**dark mica 1**	**dark mica 2**	**721r dark mica 2**	**dark mica 3**	**dark mica 3**	**dark mica 4**	**dark mica 4**
Li	**6**	3174.60	4539.10	2858.96	3803.39	3007.11	555.94	602.63	3080.80	2445.27
Li	**7**	5035.83	5301.48	3991.14	4060.62	3456.09	BD	BD	3038.13	BD
Be	**9**	4.14	2.95	7.24	6.63	5.21	6.77	6.30	18.82	19.64
Sc	**45**	121.66	95.73	74.63	119.64	142.65	250.42	259.17	79.97	97.60
Cr	**53**	76.25	113.96	120.15	51.61	61.61	148.44	115.28	56.23	103.91
Zn	**67**	736.22	646.03	669.86	620.05	583.56	1186.40	1003.91	407.11	442.05
Ga	**69**	180.93	142.50	135.69	162.44	125.46	226.33	175.28	82.00	93.38
Rb	**85**	3568.66	2675.97	3159.60	2549.48	2998.70	6252.62	6387.50	3091.84	3406.57
Sr	**88**	1.47	2.06	1.66	2.74	2.30	15.98	3.39	1.82	2.34
Y	**89**	0.01	BD	0.03	0.04	0.07	29.07	0.38	0.02	14.09
Zr	**90**	0.97	1.07	1.05	0.35	3.12	2.72	101.97	0.47	2697.90
Nb	**93**	72.73	33.17	37.71	17.90	58.28	31.64	20.27	10.61	22.03
Mo	**97**	BD	0.55	BD	BD	BD	BD	BD	0.08	BD
Cd	**111**	0.23	BD	0.21	BD	BD	1.02	BD	0.34	0.31
In	**115**	0.54	0.43	0.42	0.62	0.66	1.95	2.07	0.29	0.64
Sn	**118**	93.32	94.69	98.35	119.95	112.53	355.43	359.40	57.25	117.92
Cs	**133**	28.02	20.95	23.32	18.79	24.39	44.65	49.73	16.45	18.18
La	**139**	0.01	0.02	0.01	0.04	BD	23.53	0.02	BD	0.04
Ce	**140**	BD	0.03	0.00	BD	BD	69.76	0.08	0.00	0.50
Pr	**141**	BD	0.01	BD	BD	BD	11.29	0.02	BD	BD
Nd	**146**	BD	0.04	BD	BD	BD	43.40	BD	BD	0.19
Sm	**147**	BD	BD	0.05	0.04	BD	15.54	BD	BD	0.72
Eu	**151**	BD	0.01	0.03	BD	BD	2.56	0.02	BD	0.07
Gd	**157**	BD	BD	BD	0.13	BD	10.13	BD	0.09	1.48
Tb	**159**	BD	BD	BD	0.00	BD	1.77	BD	BD	0.51
Dy	**163**	BD	BD	0.04	BD	0.05	8.37	0.15	BD	2.26
Ho	**165**	BD	BD	BD	0.00	0.01	1.37	0.03	BD	0.62
Er	**166**	BD	BD	0.01	BD	BD	4.02	0.03	BD	2.48
Tm	**169**	BD	BD	0.00	BD	BD	0.77	BD	0.01	0.43
Yb	**172**	BD	BD	BD	0.02	BD	6.52	0.15	BD	4.28

Lu	**175**	0.00	0.01	BD	BD	BD	0.93	0.01	0.00	0.70
Hf	**178**	0.07	0.07	0.05	0.04	0.07	0.14	3.68	0.06	97.27
Ta	**181**	3.28	1.45	1.79	1.02	3.24	1.30	0.69	0.34	0.88
W	**183**	1.12	2.80	1.05	0.90	0.83	5.97	5.90	1.88	65.37
Th	**232**	BD	0.01	BD	BD	0.01	0.62	0.05	BD	8.85
U	**238**	0.13	0.14	0.12	0.15	0.12	0.52	0.65	0.12	12.01

		721r dark mica 4	**dark mica 1**	**dark mica 1**	**dark mica 1**	**722r dark mica 3**	**dark mica 3**	**dark mica 2**	**dark mica 2**
Li	**6**	5048.43	4283.77	974.09	821.36	603.29	1093.61	1090.54	1117.28
Li	**7**	BD	4328.40	447.04	444.39	486.79	483.68	570.70	592.38
Be	**9**	7.40	18.91	6.61	8.46	4.10	5.37	5.59	4.66
Sc	**45**	104.48	551.57	403.20	385.93	366.21	338.52	363.45	330.63
Cr	**53**	85.07	BD	BD	4.53	BD	BD	BD	BD
Zn	**67**	557.98	1994.59	1150.05	1481.02	800.57	756.91	792.59	674.80
Ga	**69**	86.89	244.43	73.73	319.18	78.39	85.70	97.16	94.57
Rb	**85**	3618.77	6050.56	1404.15	1654.56	4337.13	3760.04	5508.74	5525.69
Sr	**88**	1.31	0.58	0.40	3.96	1.30	BD	1.10	1.13
Y	**89**	0.05	0.28	0.03	3.01	1.18	0.09	0.37	0.30
Zr	**90**	0.30	1.03	0.43	0.67	1.10	0.21	0.61	0.65
Nb	**93**	19.78	175.01	172.93	102.41	139.74	162.31	183.85	195.76
Mo	**97**	0.59	0.66	0.18	BD	BD	BD	BD	BD
Cd	**111**	0.65	0.18	0.22	0.50	0.31	BD	0.39	0.58
In	**115**	BD	1.77	1.48	1.15	1.34	0.85	2.32	2.34
Sn	**118**	89.01	142.94	184.07	99.67	278.21	211.56	420.77	487.00
Cs	**133**	25.11	89.36	9.04	16.66	47.52	43.89	46.75	51.66
La	**139**	BD	0.12	0.02	0.42	0.21	0.05	0.26	0.39
Ce	**140**	BD	0.27	0.02	1.21	0.71	0.08	0.54	0.50
Pr	**141**	0.01	0.02	0.02	0.23	0.12	BD	0.06	0.08
Nd	**146**	BD	0.15	0.02	0.82	0.44	BD	0.11	0.34
Sm	**147**	BD	0.13	BD	0.29	0.25	BD	0.07	BD
Eu	**151**	0.02	0.02	0.01	0.05	BD	0.03	BD	BD
Gd	**157**	BD	BD	BD	0.27	BD	0.03	BD	BD
Tb	**159**	BD	0.01	0.01	0.08	0.03	BD	BD	BD
Dy	**163**	BD	BD	0.01	0.35	0.23	0.02	BD	0.03
Ho	**165**	BD	0.00	0.01	0.11	0.07	BD	BD	0.02
Er	**166**	BD	BD	0.01	0.32	0.10	BD	BD	BD
Tm	**169**	0.01	0.01	0.02	0.07	0.04	0.00	BD	0.02
Yb	**172**	BD	0.05	0.03	0.54	0.12	0.02	BD	0.18
Lu	**175**	0.01	0.01	0.01	0.07	0.02	0.01	0.02	0.02
Hf	**178**	0.09	0.36	0.18	0.13	0.10	0.06	0.10	0.20
Ta	**181**	0.13	3.06	6.41	1.84	28.56	26.65	9.63	9.27
W	**183**	1.97	2.49	0.17	2.29	2.85	1.52	14.03	15.86

Th	**232**	BD	0.01	0.00	0.27	1.23	0.02	0.05	0.23
U	**238**	0.09	0.52	0.29	4.70	2.44	0.41	2.02	1.52

		722r				**723r**				
		dark mica 4	**dark mica 4**	**light mica 1**	**light mica 1**	**dark mica 6**	**dark mica 6**	**dark mica 5**	**dark mica 5**	**dark mica 3**
Li	**6**	1071.39	2189.20	16504.71	14605.45	351.51	334.28	1514.53	863.47	BD
Li	**7**	588.64	943.20	9640.76	8032.85	1298.06	1169.00	978.00	1054.08	410.90
Be	**9**	7.63	8.69	30.17	36.30	1.84	BD	1.76	1.51	BD
Sc	**45**	331.39	429.04	315.42	223.70	62.09	63.54	25.63	31.15	26.00
Cr	**53**	<6.32	<8.13	BD	BD	BD	20.18	BD	BD	19.01
Zn	**67**	1033.72	779.87	298.44	469.30	345.55	353.94	400.64	354.68	533.14
Ga	**69**	65.32	65.88	62.96	61.23	123.45	163.81	57.50	66.80	79.30
Rb	**85**	4575.57	4766.25	2608.90	2876.70	1414.53	1728.17	1681.83	2034.20	609.93
Sr	**88**	1.14	0.37	4.43	1.64	5.75	43.03	3.46	3.10	8.60
Y	**89**	0.99	0.13	2.16	1.21	0.96	112.30	0.19	0.03	5.00
Zr	**90**	1.65	5.25	120.46	0.66	0.10	0.71	0.21	0.11	0.40
Nb	**93**	120.11	201.60	116.13	82.41	19.42	24.23	2.96	5.48	10.03
Mo	**97**	0.08	BD	BD	BD	0.26	0.24	BD	0.19	BD
Cd	**111**	0.24	BD	BD	BD	BD	BD	BD	BD	BD
In	**115**	2.07	2.01	1.95	1.37	0.76	1.29	0.31	0.42	0.25
Sn	**118**	282.65	374.52	264.63	186.36	58.72	77.04	33.54	43.68	33.03
Cs	**133**	53.57	32.47	22.91	30.80	26.59	11.41	8.45	13.04	5.74
La	**139**	0.10	0.01	0.47	0.38	36.72	1230.26	0.05	0.02	2.37
Ce	**140**	0.36	0.03	1.03	1.38	44.62	2166.79	0.07	0.02	4.32
Pr	**141**	0.07	0.00	0.15	0.14	4.24	256.02	BD	0.01	0.41
Nd	**146**	0.27	0.03	0.36	0.23	16.81	935.51	0.11	BD	2.07
Sm	**147**	0.23	0.02	0.07	0.06	2.30	132.07	0.10	BD	0.19
Eu	**151**	0.01	BD	BD	BD	0.22	23.99	0.02	BD	0.06
Gd	**157**	0.18	BD	0.16	BD	1.29	83.35	0.03	BD	0.31
Tb	**159**	0.01	BD	0.04	0.03	0.17	7.73	0.02	BD	0.07
Dy	**163**	0.05	0.02	0.30	0.31	0.41	31.40	0.13	BD	1.16
Ho	**165**	0.02	0.00	0.09	0.06	0.03	4.24	BD	0.01	0.28
Er	**166**	0.05	0.01	0.39	0.11	0.08	6.59	0.03	0.02	0.52
Tm	**169**	0.02	0.00	0.11	0.07	BD	0.65	0.02	BD	0.10
Yb	**172**	0.10	0.07	1.38	0.54	0.15	2.38	0.05	BD	BD
Lu	**175**	0.01	0.02	0.28	0.06	BD	0.16	0.01	0.02	0.13
Hf	**178**	0.19	0.67	13.04	0.10	BD	0.03	BD	BD	BD
Ta	**181**	12.78	17.80	15.55	9.00	1.23	2.06	0.30	0.29	0.53
W	**183**	5.86	11.69	18.41	32.73	0.86	2.12	2.24	4.65	17.15
Th	**232**	0.63	0.20	3.64	3.22	1.30	32.61	0.05	0.04	0.71
U	**238**	1.97	1.22	10.85	2.40	0.08	2.36	0.04	0.06	0.17

723r

		dark mica 3	dark mica 4	dark mica 4	dark mica 1	dark mica 1
Li	**6**	BD	361.85	387.54	693.43	1010.42
Li	**7**	589.39	709.28	667.78	664.37	656.64
Be	**9**	BD	3.78	1.35	3.61	BD
Sc	**45**	33.44	49.62	50.65	20.26	32.08
Cr	**53**	24.14	23.70	29.97	BD	BD
Zn	**67**	510.18	445.40	387.00	471.38	530.15
Ga	**69**	96.22	182.38	151.26	71.52	111.55
Rb	**85**	1065.33	2152.94	2183.70	982.52	2321.05
Sr	**88**	11.78	7.57	4.93	5.13	6.75
Y	**89**	1.83	2.91	0.42	0.03	0.04
Zr	**90**	1.58	3.03	6.95	4.99	3.71
Nb	**93**	84.10	113.26	300.96	12.14	27.54
Mo	**97**	0.70	0.64	0.22	0.78	BD
Cd	**111**	BD	BD	BD	BD	BD
In	**115**	0.33	0.87	0.76	0.69	0.69
Sn	**118**	45.54	76.18	103.98	110.02	136.05
Cs	**133**	10.37	15.86	20.15	7.96	22.79
La	**139**	1.00	1.69	0.13	0.04	0.07
Ce	**140**	1.87	3.18	1.04	BD	0.07
Pr	**141**	0.35	0.31	BD	BD	BD
Nd	**146**	0.52	1.37	0.41	BD	0.06
Sm	**147**	0.09	0.34	0.06	BD	BD
Eu	**151**	0.11	0.19	0.02	0.02	0.05
Gd	**157**	0.10	0.54	BD	0.03	0.05
Tb	**159**	0.02	0.11	0.02	BD	0.01
Dy	**163**	0.40	0.25	0.13	0.14	BD
Ho	**165**	0.06	0.06	0.04	0.01	0.01
Er	**166**	0.18	0.49	0.07	BD	0.02
Tm	**169**	0.03	0.03	0.01	0.01	BD
Yb	**172**	0.16	0.40	0.06	BD	0.07
Lu	**175**	0.03	0.07	BD	BD	0.01
Hf	**178**	0.09	0.26	0.36	0.19	0.10
Ta	**181**	4.66	5.81	8.33	1.81	4.06
W	**183**	53.23	61.47	119.69	2.68	5.51
Th	**232**	0.82	0.90	0.57	BD	BD
U	**238**	0.86	1.25	2.46	0.08	0.07

Mica analyses performed via LA-ICP-MS. BD represents values that were below the detection limit of the instrument. In parts per million (ppm).

Appendix C: F-test and t-tests

MP vs Tpz-rhy Zr

F-Test Two-Sample for Variances

	Tpz-rhy	MP
	Variable 1	*Variable 2*
Mean	4.903227316	0.343798001
Variance	5.123485277	0.073180585
Observations	22	15
df	21	14
F	70.01153725	
P(F<=f) one-tail	9.20604E-11	
F Critical one-tail	2.376811932	

DIFFERENT

t-Test: Two-Sample Assuming Unequal Variances

	Tpz-rhy	MP
	Variable 1	*Variable 2*
Mean	4.903227316	0.343798001
Variance	5.123485277	0.073180585
Observations	22	15
Hypothesized Mean Difference	0	
df	22	
t Stat	9.350548184	
P(T<=t) one-tail	2.01874E-09	
t Critical one-tail	1.717144374	
P(T<=t) two-tail	4.03749E-09	
t Critical two-tail	2.073873068	

MP vs Climax Zr

F-Test Two-Sample for Variances

	Climax	MP
	Variable 1	*Variable 2*
Mean	1.663035796	0.343798001
Variance	3.473240044	0.073180585
Observations	24	15
df	23	14
F	47.46122249	
P(F<=f) one-tail	1.16053E-09	
F Critical one-tail	2.357306178	

DIFFERENT

t-Test: Two-Sample Assuming Unequal Variances

	Climax	MP
	Variable 1	*Variable 2*
Mean	1.663035796	0.343798001
Variance	3.473240044	0.073180585
Observations	24	15
Hypothesized Mean Difference	0	
df	25	
t Stat	3.410841853	
P(T<=t) one-tail	0.0011032	
t Critical one-tail	1.708140761	
P(T<=t) two-tail	0.0022064	
t Critical two-tail	2.059538553	

Tpz-rhy vs Climax Zr

F-Test Two-Sample for Variances

	Tpz-rhy	Climax
	Variable 1	*Variable 2*
Mean	4.903227316	1.663035796
Variance	5.123485277	3.473240044
Observations	22	24
df	21	23
F	1.475131351	
P(F<=f) one-tail	0.182254863	
F Critical one-tail	2.035632573	

DIFFERENT

t-Test: Two-Sample Assuming Equal Variances

	Tpz-rhy	Climax
	Variable 1	*Variable 2*
Mean	4.903227316	1.663035796
Variance	5.123485277	3.473240044
Observations	22	24
Pooled Variance	4.260857087	
Hypothesized Mean Difference	0	
df	44	
t Stat	5.318145837	
P(T<=t) one-tail	1.67503E-06	
t Critical one-tail	1.680229977	
P(T<=t) two-tail	3.35006E-06	

t Critical two-tail	2.015367574

MP vs Tpz-rhy La

F-Test Two-Sample for Variances

	Tpz-rhy	MP
	Variable 1	*Variable 2*
Mean	0.997520522	0.040885431
Variance	1.374373911	0.003748969
Observations	22	15
df	21	14
F	366.6005484	
P(F<=f) one-tail	9.58987E-16	
F Critical one-tail	2.376811932	

DIFFERENT

t-Test: Two-Sample Assuming Unequal Variances

	Tpz-rhy	MP
	Variable 1	*Variable 2*
Mean	0.997520522	0.040885431
Variance	1.374373911	0.003748969
Observations	22	15
Hypothesized Mean Difference	0	
df	21	
t Stat	3.81977854	
P(T<=t) one-tail	0.000499403	
t Critical one-tail	1.720742903	
P(T<=t) two-tail	0.000998806	
t Critical two-tail	2.079613845	

MP vs Climax La

F-Test Two-Sample for Variances

	Climax	MP
	Variable 1	*Variable 2*
Mean	0.293568849	0.040885431
Variance	0.344108338	0.003748969
Observations	24	15
df	23	14
F	91.78747103	
P(F<=f) one-tail	1.2665E-11	
F Critical one-tail	2.357306178	

DIFFERENT

t-Test: Two-Sample Assuming Unequal Variances

	Climax	MP
	Variable 1	*Variable 2*
Mean	0.293568849	0.040885431
Variance	0.344108338	0.003748969
Observations	24	15
Hypothesized Mean Difference	0	
df	24	
t Stat	2.092098657	
P(T<=t) one-tail	0.023592265	
t Critical one-tail	1.71088208	
P(T<=t) two-tail	0.04718453	
t Critical two-tail	2.063898562	

Tpz-rhy vs Climax La

F-Test Two-Sample for Variances

	Tpz-rhy	Climax
	Variable 1	*Variable 2*
Mean	0.997520522	0.293568849
Variance	1.374373911	0.344108338
Observations	22	24
df	21	23

t-Test: Two-Sample Assuming Unequal Variances

	Tpz-rhy	Climax
	Variable 1	*Variable 2*
Mean	0.997520522	0.293568849
Variance	1.374373911	0.344108338
Observations	22	24
Hypothesized Mean Difference	0	

F	3.994015134
P(F<=f) one-tail	0.00087649
F Critical one-tail	2.035632573

DIFFERENT

df	30
t Stat	2.540011546
P(T<=t) one-tail	0.008250448
t Critical one-tail	1.697260887
P(T<=t) two-tail	0.016500896
t Critical two-tail	2.042272456

MP vs Tpz-rhy Lu

F-Test Two-Sample for Variances

	MP	**Tpz-rhy**
	Variable 1	*Variable 2*
Mean	0.095745627	0.039335118
Variance	0.082732094	0.001366591
Observations	15	22
df	14	21
F	60.53903712	
P(F<=f) one-tail	9.28163E-14	
F Critical one-tail	2.197472626	

SIMILAR

t-Test: Two-Sample Assuming Unequal Variances

	MP	**Tpz-rhy**
	Variable 1	*Variable 2*
Mean	0.095745627	0.039335118
Variance	0.082732094	0.001366591
Observations	15	22
Hypothesized Mean Difference	0	
df	14	
t Stat	0.755329937	
P(T<=t) one-tail	0.231285109	
t Critical one-tail	1.761310136	
P(T<=t) two-tail	0.462570218	
t Critical two-tail	2.144786688	

MP vs Climax Lu

F-Test Two-Sample for Variances

	MP	**Climax**
	Variable 1	*Variable 2*
Mean	0.095745627	0.020683766
Variance	0.082732094	0.000965094
Observations	15	23
df	14	22
F	85.72443117	
P(F<=f) one-tail	7.20356E-16	
F Critical one-tail	2.172694693	

SIMILAR

t-Test: Two-Sample Assuming Unequal Variances

	MP	**Climax**
	Variable 1	*Variable 2*
Mean	0.095745627	0.020683766
Variance	0.082732094	0.000965094
Observations	15	23
Hypothesized Mean Difference	0	
df	14	
t Stat	1.006890382	
P(T<=t) one-tail	0.165537054	
t Critical one-tail	1.761310136	
P(T<=t) two-tail	0.331074107	
t Critical two-tail	2.144786688	

Tpz-rhy vs Climax Lu

F-Test Two-Sample for Variances

t-Test: Two-Sample Assuming Equal Variances

Tpz-rhy	**Climax**

Tpz-rhy	**Climax**

	Variable 1	*Variable 2*
Mean	0.039335118	0.020683766
Variance	0.001366591	0.000965094
Observations	22	23
df	21	22
F	1.416019072	
P(F<=f) one-tail	0.212036612	
F Critical one-tail	2.058728407	

SIMILAR

	Variable 1	*Variable 2*
Mean	0.039335118	0.020683766
Variance	0.001366591	0.000965094
Observations	22	23
Pooled Variance	0.001161174	
Hypothesized Mean Difference	0	
df	43	
t Stat	1.835400107	
P(T<=t) one-tail	0.036684411	
t Critical one-tail	1.681070703	
P(T<=t) two-tail	0.073368822	
t Critical two-tail	2.016692199	

MP vs Tpz-rhy Xannite

F-Test Two-Sample for Variances

	Tpz-rhy	MP
Mean	*Variable 1*	*Variable 2*
Variance	0.535541252	0.337024951
Observations	0.016946922	0.00018455
df	31	26
F	30	25
P(F<=f) one-tail	91.82818812	
F Critical one-tail	3.30304E-19	
	1.91918774	

DIFFERENT

t-Test: Two-Sample Assuming Unequal Variances

	Tpz-rhy	MP
	Variable 1	*Variable 2*
Mean	0.535541252	0.337024951
Variance	0.016946922	0.00018455
Observations	31	26
Hypothesized Mean Difference	0	
df	31	
t Stat	8.435878022	
P(T<=t) one-tail	7.88255E-10	
t Critical one-tail	1.695518783	
P(T<=t) two-tail	1.57651E-09	
t Critical two-tail	2.039513446	

MP vs Climax Xannite

F-Test Two-Sample for Variances

	Climax	MP
Mean	*Variable 1*	*Variable 2*
Variance	0.338620674	0.337024951
Observations	0.002050388	0.00018455
df	29	26
F	28	25
P(F<=f) one-tail	11.11018259	
F Critical one-tail	2.29308E-08	
	1.932294679	

SIMILAR

t-Test: Two-Sample Assuming Unequal Variances

	Climax	MP
	Variable 1	*Variable 2*
Mean	0.338620674	0.337024951
Variance	0.002050388	0.00018455
Observations	29	26
Hypothesized Mean Difference	0	
df	34	
t Stat	0.180910817	
P(T<=t) one-tail	0.428755847	
t Critical one-tail	1.690924255	
P(T<=t) two-tail	0.857511693	
t Critical two-tail	2.032244509	

Tpz-rhy vs Climax Xannite

F-Test Two-Sample for Variances

	Tpz-rhy	Climax
Mean	*Variable 1*	*Variable 2*
Variance	0.535541252	0.338620674
Observations	0.016946922	0.002050388
df	31	29
F	30	28
P(F<=f) one-tail	8.265227628	
F Critical one-tail	1.22708E-07	
	1.868709158	

DIFFERENT

t-Test: Two-Sample Assuming Unequal Variances

	Tpz-rhy	Climax
	Variable 1	*Variable 2*
Mean	0.535541252	0.338620674
Variance	0.016946922	0.002050388
Observations	31	29
Hypothesized Mean Difference	0	
df	38	
t Stat	7.925297151	
P(T<=t) one-tail	7.14236E-10	
t Critical one-tail	1.68595446	
P(T<=t) two-tail	1.42847E-09	
t Critical two-tail	2.024394164	

"I pledge on my honor that I have not given or received any unauthorized assistance or plagiarized on this assignment."